UiT
THE ARCTIC
UNIVERSITY
OF NORWAY

Faculty of Science and Technology
Department of Geology

Hydrothermal vent Activities At the Gjallar Ridge In the Vøring Basin, mid-Norway

Isaac Njone
Master's thesis in Geology (GEO-3900)
November 2014

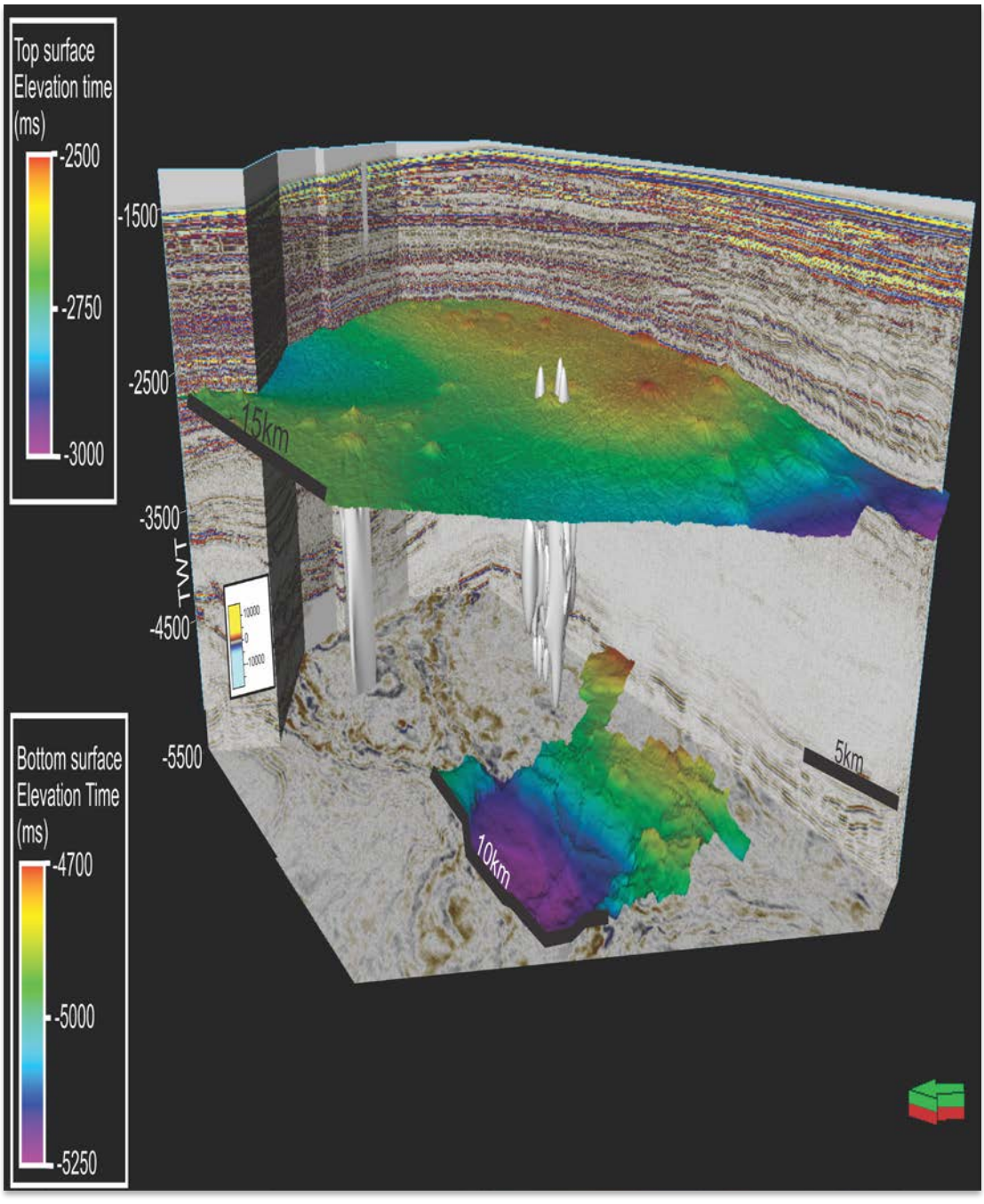

Abstract

The 3D seismic enable a better understanding of phreatomagmatic activity that occurred at the Gjallar ridge in the Vøring basin, mid-Norway. Structures associated with this activity were imaged and a causality relationship was established. Those structures included hydrothermal vent complexes, sill complexes and faults. The Kai formation significantly affected by polygonal faulting that were likely to play as evacuation structures for the fluid migrating to the BPU.

Key words: Hydrothermal and sill complexes, Polygonal faults.

Acknowledgement

I would like to use this opportunity to express my deepest acknowledgement to all those whose supported me during my stay as a student at the arctic university of Norway, Tromsø and those without whom I would have not completed this master's thesis. I am very grateful to my supervisors Stefan Buenz and Juergen Mienert who gave me this opportunity. I am also indebted to my family for their love and support. I wouldn't forget my classmates and friends Yoanes, Robert and petter and Bjani with whom I shared this stressfull moment.

Contents

1 INTRODUCTION

1.1 Objectives

The overall aim of this master's thesis is to better understand the hydrothermal activity at the Gjallar Ridge by use of 3D seismic data. The primary objectives include the identification and mapping of hydrothermal vent complexes, the identification of sill complexes and the establishment of their implication in the fluid flow in the study area.

1.2 Introduction to volcanic intrusion

Magma cooling and solidification before it reaches the surface lead to igneous intrusion formation. Three common types of intrusions include dykes, sills and batholiths.

Sill occurences in seismic data

Initiation on seismic sections is based on their tendency to cross-cut stratigraphy and their high seismic amplitudes. The gross geometry, size and location of sills can be determined by this means along with the geometry sill-sill contacts.

Sill complex geometries

Radially symmetrical and consists of a saucer-like flat inner sill at the base with an arcuate inclined sheet connecting it to gently inclined, commonly ragged, outer rim. Geometries that previously have been documented using 3D seismic data form the Faroe-Shetland Basin (Davies et al., 2002 Smallwood and Maresh 2002) and classic onshore localities (mention the importance of such outcrop) such as the Karoo of South Africa (Du Toit 1920; Chevalier and Woodford 1999), the Whin Sill (Francis 1982; Johnson and Dunham 2001), the Midland Valley Sill (Francis 1982) and in Tasmania (Leaman 1975).

Within a sill complex the seismic data also demonstrate that the inclined sheet consists of a series of concave inwards segments providing the cuspate geometry also seen in the Karoo sills (Chevalier and Woodford 1999) and the Rockall Through (Hutton and Thomson, 2003)

By means of conventional seismic several sill types can be recognized in sedimentary basins, exhibiting complex internal architectures.

Saucer-shape sills previously have been documented in classic onshore localities such as the Karoo in South Africa (Du Toit, 1920; Chevalier and Woodford, 1999), the Whin Sill (Francis 1982; Johnson and Dunham, 2001), the Midland Valley Sill (Francis, 1982) and in Tasmania (Leaman, 1975) as well as by the means of 3D seismic data from the Faroe-Shetland basin

(Davies et al., 2002; Smallwood and Maresh, 2002) and the North Rockall Trough (Thomson and Hutton, 2004).

Hybrid geometries involve multiple inner saucers, outer rims and inclined sheets.

Branching relationships are interpreted as magma flow channels within the sheet (Thomson and Hutton, 2003).

Elongate, bilaterally symmetrical sill complexes also can be found within the North Rockall Trough.

Cuspate geometry of the incline sheets:

With an average length of around 3 km, and a width of 1 km, each primary flow unit is fed by a primary magma tube, generally elongated in the direction of propagation (i.e. towards the sill complex periphery) and has a slightly concave upwards cross section normal to the direction of propagation.

Sill merger and development of Junctions

The merging of sill complexes to form hybrid sill complexes, or the merger of flow units within a sill complex, results in the development of junctions due to the abutment of a sill or sill complex against a second sill or sill complex (Thompson & Hutton 2003). Merging sill complexes to form hybrid sill complexes usually results in the development of inclined and antiformal junctions (Thompson & Hutton 2003).

The inclined junction evolvement is due to the abutment of an inclined sheet of an adjacent sill complex. Antiformal junctions develop between the tips of two inclined sheets from adjacent sill complexes. Unlike inclined junctions, both of the inclined sheets are equally developed and merge to form a tight antiformal closure with neither inclined sheet continuing upwards to form an outer rim (Fig.1.2.2).

Flow indicator structures within sill complexes

Although junctions mark the limits of flow units within both simple sill complexes and hybrid sill complexes, a number of structures can be found within sill complexes that place constraints on magma flow directions.

Models of sill emplacement

The North Rockall Trough provides data that suggests that the feeder of the sill complex is connected to the inner saucer. Dykes have been identified as the principal source of sill complexes on the basis of of outcop observations (Thomson and Hutton, 2003). As a result, an alignment of sill complexes corresponding to the preferred dyke orientation across the region would be expected.

Four basic mechanisms for doleritic sill intrusion have been proposed, mainly based on outcrop studies : (1) the concept of “compensation”, sill intrude at depths where the magma pressure equals the lithostatic pressure (Bradley, 1965); (2) the concept of magma overshoot and gravitational flow where an ascending feeder dyke overshoots the optimum level for lateral intrusion (Bradley, 1965); the development of the Whin and Midland Valley sills, northern Britain , has been explained by Francis (1982) using these concepts. (3) Ring dyke model of Chevalier and Woodford (1999) suggests that an ascending ring dyke begins to develop a flatter outer rim, wits inflation gradually lifting the country rock overlying the ring dyke. Uplift of the block subsequently allows the downward migration of magma into the area contained within the ring dyke, leading to the development of a flat inner sill within the confines of the ring dyke (Fig. 1.2.1c). This model was developed for Karoo sills. (4) The model of Pollard and Johnson (1973) developed for the diorite sills and laccoliths of the Henry Mountains, Utah, assuming that the sill overlies a central feeder and that the inner saucer thickens sufficiently to result in roof uplift and radial peripheral fracturing and dyking. The emplacement the Karoo sills could be explained using this model (Burger et al, 1981) which is also compatible with the observations from the North Rockall Trough (Thompson and Hutton, 2003).

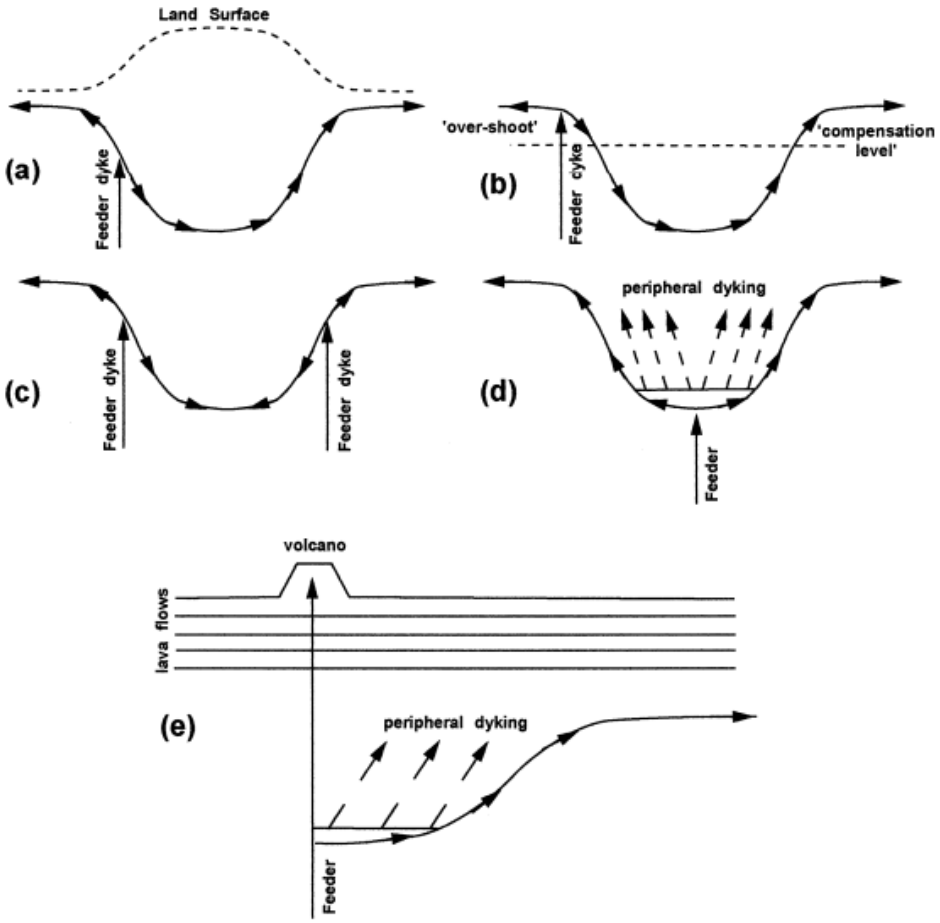

Figure 1.2.1 Models for radially symmetrical sill growth. (a) The concept of a compensation surface mirroring topography (Bradley 1965). (b) magma overshoot and gravitational flow (Francis 1982). (c) the ring dyke model (Chevalier and Woodford 1999). (d) this study and Burger et al. (1981): are centrally sourced laccolith model with peripheral dyking. (e) model for volcano related, bilaterally symmetrical, sills based on (d).

Formation of Sediment pipes and dykes

A variety of pressure build-up mechanisms might be the cause of both sediment pipes and dykes formation (Lowe 1975; Hannum 1980; Guhman and Pederson 1992; Kenkman 2003; Shoulders & Cartwright 2004; Jamveit et al. 2004; Svensen et al. 2006). These mechanisms include overpressured clastic beds with brines or petroleum (Lowe 1975; Hannum 1980; Mount 1993; Shoulders & cartwright 2004), flow of ground water (Guhman & Pedersen 1992) impact cratering (Kenkmann, 2003), and boiling (Jamtveit et al. 2004).

The fluidization (transport of granular material in a fluid) occurring during phreatic explosive events have minimum velocities in pipes that are of the order of several hundred metres per

second (Nvikov & Slobodskoy, 1979; Zimanowski et al. 1991; Kurszlaukis et al. 1998; Boorman et al. 2003).

1.3 Introduction to fluid flow Hydrothermal venting

Fluid generation is arguably the most prominent and common activity involving both geological and microbiological processes. The fluids derived from these processes may be generated close to the seabed or distant both in time and space. The nature of fluids flowing through the sedimentary sequences and seabed varies in terms of their physical properties and origin and thus include liquid and gas that might be organic or inorganic.

The formation of hydrothermal fluids result from hot rocks and pore fluid interaction under igneous processes' influence (Judd & Hovland, 2007). Hydrocarbons, stemmed from organic matter degradation, remain the most prominent fluids generated within sedimentary basins. Methane is regarded as the main hydrocarbon generated within the sediments as a result of either micro-organisms' activity, termed biogenic or microbial, or processes occurring deeper within the sedimentary sequences and known as thermogenic.

Fluids generated during sediment burial experiences various fate determined by geological conditions and physical conditions of the area. The migration of fluids is fostered by buoyancy through the sedimentary sequences. Fluids are prone to be either seeping throughout the surface or trapped when the geological and physical conditions are met. Geological traps consist one the means by which fluids are accumulated at different depths in the sedimentary formations. The second means that leads to fluid accumulation, especially methane, is the gas hydrate formation under relevant conditions of both temperature and pressure in deep sea. Seabed morphological features such as pockmarks and others subseabed features (gas chimney, mud diapirs, mud volcanoes, diatremes) always form as a result of migration mechanism (Judd & Hovland, 2007).

Geological phenomena that are involved in the production and migration of fluid throughout geological formations on one hand and associated features on the second hand encompass volcanic activity, geothermic gradient and water Flows.

Various gases are released in the atmosphere as a result of geological activity. Cooled and solidified magma comprise gas bubbles or frozen vesicles. It's also unambiguous that bubbles' explosion during volcanic events illustrate gas abundance in the magma. Gases involved in volcanic activities include CO_2, HCl, SO_2 and H_2O (water vapour); Hydrothermal venting releases gases such as H_2, CO, NO_2 and CO_2 while He and Rn stem from magma (Judd & Hovland, 2007).

Volcanic activity generally involves magma with high temperatures comprised between 700^{o} C and 1300^{O} C. However this temperature range becomes larger when a mixture of molten rock such as carbonatites, that may be as cool as 600^{o} C, and komatiites, that might have been as hot as 1600^{o} C, are taken into consideration (Bottinga and Weill, 1972). The buoyancy of fluids is so prominent at such high temperatures that fluid migration associated to volcanic activity might continue when the volcanoes are already dormant.(Judd & Hovland). The evolvement of magma in it composition as it cools is due to the progressive crystallization of minerals at specific temperatures. The presence of fluid inclusions, within crystals of rock-forming minerals, illustrates the presence of compounds formed as minerals that crystallized earlier reacts with the melt as the magma cools down. Although methane is less abundant, compared with other fluids such as carbon dioxide, water or monoxide, three situations in which it synthetized were identified by Apps and van de Kamp (1993) as follows: (1) Degassing and / or cooling of mafic magma at spreading centres. The most abundant gases are carbon dioxide and hydrogen sulphide, the presence of methane is also notable. These gases are amongst the fluids emitted by hydrothermal vents. (2) serpentinisation of ultramafic rocks (peridotite). The rise of methane-rich plumes into the water column and diapiric serpentinite bodies identification show that this process occurs near spreading centres and near subduction zones (3) Layered mafic intrusions' cooling. "Potholes", consist of high pressure gas (hydrogen and hydrogen sulphide), are pockmark-like evidence of rise of fluids through the crystals sinking at the magma chamber. They can be found on continental margins and likely formed during early stages of continental rifting.

Geothermal systems

Hydrothermal circulation systems

The heat of Earth's interior is thought to have several sources. Apart from the heat derived from the formation of the planet, the earth-interior's heat is generated by natural decay of radioactive isotopes of elements including potassium-40, uranium-235 and thorium-232 in the mantle and rocks of the Earth's crust. The temperature resulting from this heat increases with depth in the earth's interior. The rate of that increase is termed as geothermal gradient. Plate boundaries as well as sites of cooling igneous intrusions constitute ideal places for crustal thinning occurrence. On land, hot springs, fumaroles and Geysers occur within these places. On the contrary the occurrence of submarine springs within the same places is apparently seldom since their appearance and acoustic signal are similar to those of hydrothermal (mineral-rich) and cold freshwater seeps (Judd & Hovland 2007).

Hydrothermal activity is triggered as water is warmed up by hot volcanic rocks and magma. Submarine volcanism is always associated with hydrothermal activity for seawater is involved in cracking, cooling and altering newly emplaced magma. Cold (2-4^{o} C), dense seawater circulate in igneous rocks, occurring in back-arc systems, many seamount environments and spreading ridges, through a 'stockwork' system including fissures, faults and wrenches. As seawater penetrates to different depth, it is heated when it flows near sills, dykes and shallow magma, and becomes buoyant. This heated seawater is chemically altered by percolated rocks. Hydrothermal vents constitute pathways that allow the resulting fluid to rise to the seabed. Minerals precipitate as a result of sudden change in ambient conditions meanwhile plumes of the remaining hydrothermal fluid migrate towards the seabed and ascend in the water column (Judd & Hovland, 2007).

The oceanic crust constitutes the greater part of the Earth's crust. It's exposition to seawater or to saturated water tremendously increases it potential for hydrothermal systems (Judd & Hovland, 2007). The permeability and porosity of the ocean crust near hydrothermal vents are remarkable. Average porosities of nearly 25% and profound fracturing in rocks affected by hydrothermal activities encountered during ODP Leg 193 drilling in the Manus Basin for instance are reported by Binns et al. (2001). The ocean crust contains a total amount of water that is constantly equivalent to ocean water (Fyfe, 1992). It takes about 10 million years to the entire ocean mass to recycle through hydrothermal vent systems (Fyfe, 1994).

Hydrothermal systems can be subdivided into three zones as follows (Butterfield, 2000) (Figure 3.1):

(1) a recharge zone, here seawater flowing down through the crust is gently warmed up and undergoes chemical alteration under low-temperature reactions; Although Places where seawater percolates down the oceanic crust are seldom, the Ocean Drilling Project (ODP) and the Deep Sea Drilling Project at site 395 in the Atlantic Ocean revealed a recharge zone where the flowing rate of water was about 1000 liters/ hr (Becker, 1998).

(2) a high temperature reaction zone, in the vicinity of the heat source, here fluid balances with hot rock; Both temperature and pressure alter seawater composition and behavior as it flows through the oceanic crust (Judd & Hovland, 2007). At temperatures of about 130-150^{o} C important changes are noticeable. The richness of seawater in sulfate anion in seawater, second largest, is so important that it chemically alter the fluid composition at temperature higher than 130-150^{o} by filling the pore spaces with precipitated anhydrite ($CaSO_4$) (Butterfield, 2000).

The precipitation of smectite and chlorite from seawater takes place as the temperature of the water body exceeds 130-150^{o} C. This process leads to depletion of significant amount of magnesium from the fluid. The scarcity of magnesium causes acidification of the remaining fluid (Judd & Hovland, 2007).

(3) an upflow zone and venting, here buoyant and heated fluids rise quickly to the seabed. Conductive heat loss, adiabatic decompression as well as contact with ambient fluids around the conduits are account amongst the factors fostering the cooling of ascending fluids in the upflow zone (Butterfield, 2000).

The migration pathway used by fluid to rise to the seabed, it insulation and the expansion to which it mixes with pore water that did not undergo heating determine the extent of cooling. The precipitation of solutes during cooling lead the change in fluid nature. For instance the precipitation of metal sulphides lead to acidification of the medium. When seawater is encountered by fluids emanating from hydrothermal activity, the colossal temperature difference in temperature causes a rapid cooling resulting in spontaneous precipitation of minerals. The hydrothermal fluids emerging through the seabed may rich temperatures comprised between 300 and 400^{o} C. At this temperature range venting fluids may occur in vapor phase, or in brine phase resulting from phase separation or in a mixture of the two (Judd & Hovland, 2007).

Reactions that result in heat liberation are termed as exothermic. The heat that is release in such reaction might be prominent in hydrothermal systems. In the divergent margins magma is the likely source of heat. However some hydrothermal fluids stemming from processes different from those occurring in rifting margins are found elsewhere (e.g. Lost City, Kelly *et al.* 2001). In these sites seawater percolating from the seabed reacts with olivine-rich rocks such as peridotites during serpentinisation. Equations (1a) and (1b) summarise these reactions (Judd & Hovland, 2007).

$5Mg_2SiO_4 + Fe_2SiO_4 + 9H_2O \rightarrow 3Mg_3Si_2O_5(OH)_4 + Mg(OH)_2 + 2Fe(OH)_2$

Forsterite Fayalite Serpentinite Brucite (1a)

$\rightarrow 3Fe(OH)_2 \rightarrow Fe_2{+}Fe_3{+}\ 2\ O_4 + H_2 + 2H_2O$

Magnetite (1b)

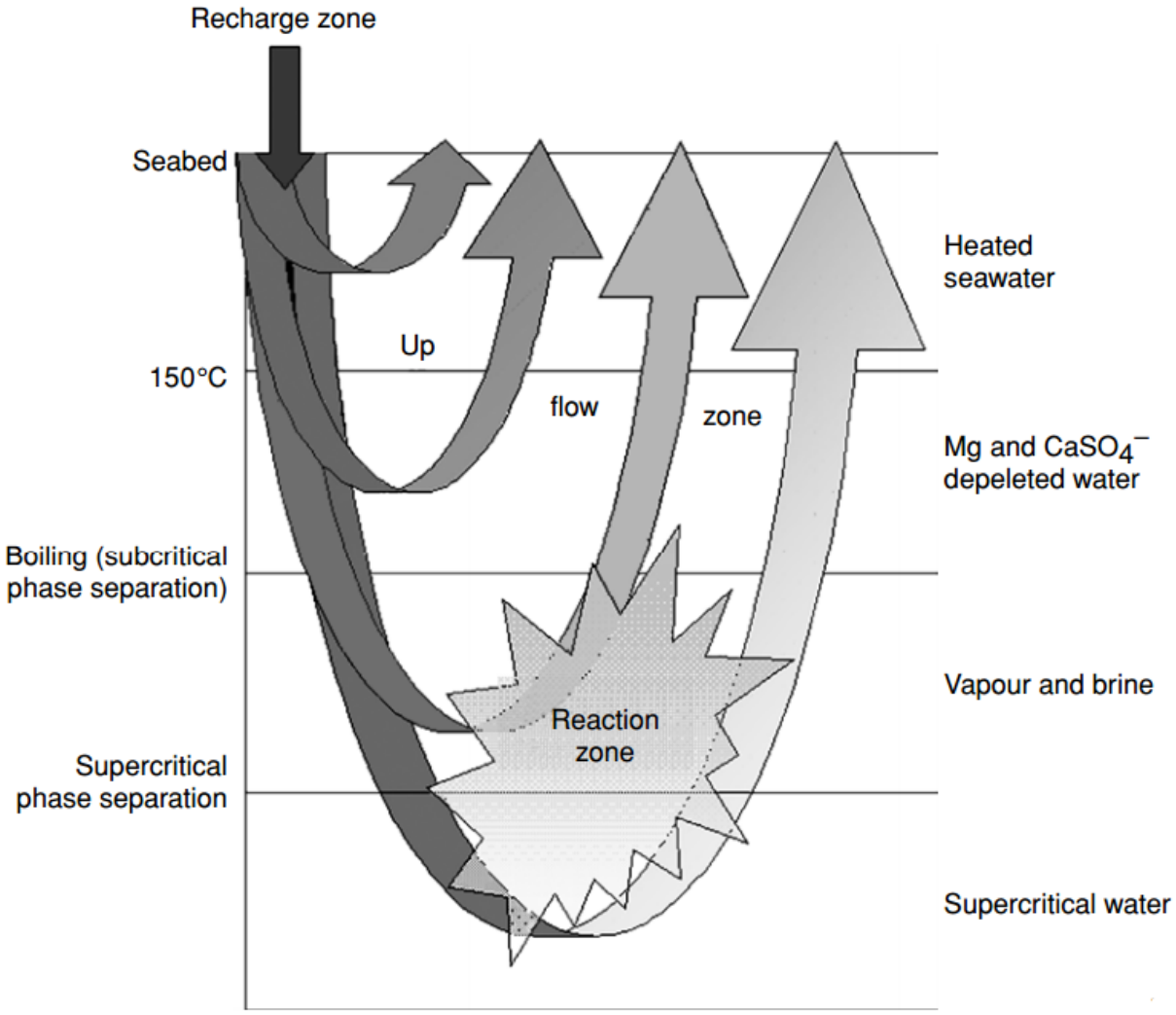

Figure. 13.1 *Cartoon showing the principal zones hydrothermal circulation systems. Threshold depths depend on water depth, geothermal gradients, and water salinity (Judd & hovland, 2007).*

Magma – induced hydrothermal vent complex

Water responds differently when it undergoes heating within a contained and uncontained volume. Pressurization is the result when contained meanwhile expansion and flowing occur subsequently within an uncontained volume (Delaney, 1982).

A causal relationship has been established between sill intrusions and hydrothermal vent complexes in volcanic basins around the world (Figures.1.3.2, 3, 4),e.g. Vøring and Møre Basins in the mid-Norwegian margin) Planke *et al.*, 2002; Svensen *et al.*, 2003; .Jamtveit *et al.*, 2004; Planke *et al.*, 2005). Though hydrothermal vents are not characteristic of volcanic basins. For instance the Australian NW Shelf is deprived of hydrothermal vents on large parts (Symonds *et al.*, 1998). The abundance of hydrothermal vents in volcanic basins is influenced

by the sills' geometry, the composition and permeability of the host-rock and the detectability of the vent complex (seismic horizontal-resolution) (Planke *et al.*, 2005).

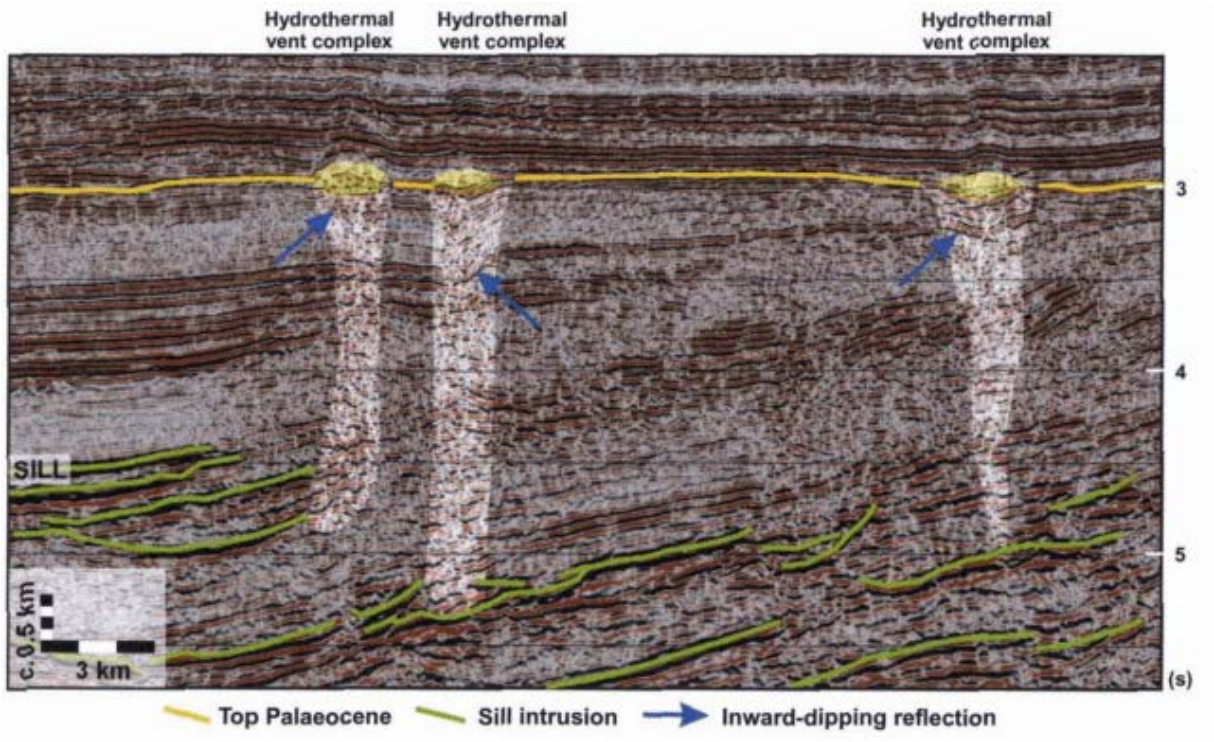

Flg. 1.3.2. *Seismic expression of three hydrothermal vent complexes cutting Palaeocene and Cretaceous clastic sedimentary strata in the north-central Vøring Basin. High-amplitude reflections are interpreted as mafic sills based on their morphology, seismic shadowing effects, aeromagnetic and well data. Note that the sedimentary strata dip into the vent (blue arrows). The vent complexes are associated with a positive perturbation of the topographic relief at the palaeosurface (yellow ellipses). These vent eye-like structures are interpreted as 'mud-volcanoes' and may reach several kilometres in diameter* (Jamtveit *et al.*, 2004).

The difference between hydrostatic pressure and local fluid pressure is *sine qua non* for the occurrence of hydrothermal vent complexes. The local fluid pressure must exceed the hydrostatic pressure (Fig. 1.3.4). This condition is only possible if the pressure builds up quicker than it releases. In other words the pressure build-up is fast and the permeability of the host-rock is small (Jamtveit *et al.*, 2004). Overpressure in the immediate vicinity of the sills may be stemmed by metamorphic reactions producing gas and/or gas expel from intruded magma or boiling of host-rock pore fluids (Planke *et al.*, 2005).

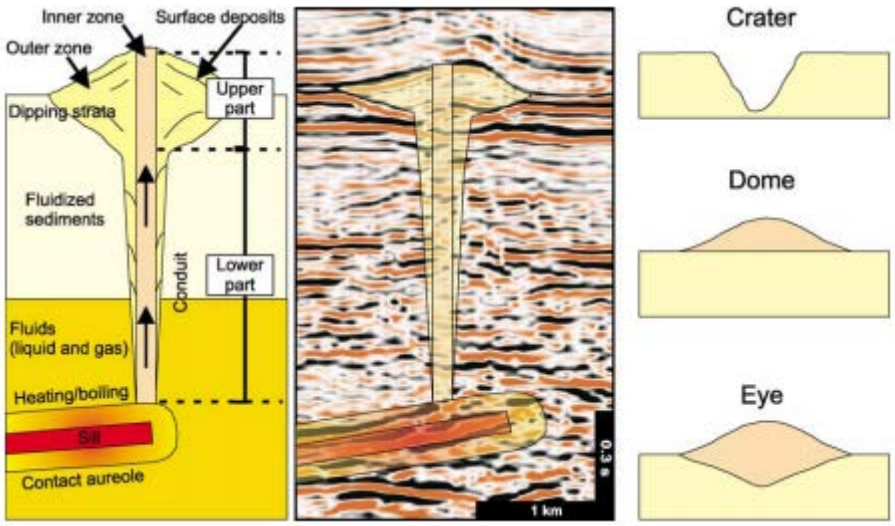

Figure 1.3.3 *Sketch and seismic example of a hydrothermal vent complex. The complex consists of an upper and a lower part. The upper part is crater-, dome- or eye-shaped and is connected to the termination of a sill by a cylindrical conduit zone with disturbed seismic data in the lower part* (Planke *et al.*, 2005).

Jamtveit *et al. (2004)* modelled fluid channeling caused by overpressure *shortly after* the sill is emplaced. The width of overpressure zone (H_{op}), at the early stages of sill cooling, is expressed by *the characteristic length scale for hydraulic diffusion:*

$$H_{OP} \approx 2\sqrt{k_{fluid} t} \tag{1}$$

Where $k_{fluid} = k/\beta\phi\mu_{fluid}$ represents the hydraulic diffusivity; $\beta \approx 10^{-8}$ Pa^{-1} the effective fluid and pore compressibility; t, the time since sill emplacement; μ_{fluid}, fluid viscosity; K, the permeability; ϕ, the porosity. The boiling zone thickness can be expressed by a similar scaling relation:

$$H_{boil} \approx 2\sqrt{k_T t} \tag{2}$$

Where $k_T \approx 10^{-6}$ m^{2}s^{-1} represents the heat diffusivity. The front velocity, V_{boil}, can therefore be expressed as:

$$V_{boil} \approx \sqrt{\frac{k_T}{t}} \tag{3}$$

Shortly after the sill emplacement, given that the volume of pore fluids stored in the rocks is still insignificant, the advective heat transport is consequently unimportant and the permeability does not influence the boiling zone thickness (Delaney 1982; Podlachnikov & Wickham 1994).

At the later stages after the sill emplacement, significant amount of fluids flowing through the same rock increase the significance of advective heat transport and fluids that were heated by the rock during sill cooling start heating the rocks in its turn (Jamtveit *et al.,* 2004).

The buoyancy of hot vapour may be significant through the boiling front, once it encounters cold rocks the condensation into water occurs without influencing the boiling front velocity (Jamtveit *et al*., 2004).

At early pressurization stage cold-water properties can be used for the overpressure zone thickness is much bigger than the boiling zone thickness. Out of the boiling zone the Darcian fluid flow can be expressed as follows:

$$Q_D \approx \frac{k}{\mu_{fluid}} \frac{P_{fluid} - P_{hyd}}{H_{OP}} \tag{4}$$

Where the difference between fluid pressure and hydrostatic pressure (the *overpressure*) is given by ($P_{fluid} - P_{hyd}$). At the early stages P_{hyd} is insignificant, thus $Q_D << V_{boil}$, steam is significantly produced enabling an increase in fluid pressure *to a slowly decaying value characterized by a quasi-static flux balance:*

$$\rho Q_D = \phi \Delta\rho_{boil} V_{boil} \tag{5}$$

Where ρ and $\Delta\rho_{boil}$ ($\approx\rho$) express the cold-water density and the density difference between supercritical steam and cold water. The hydrostatic fluid pressure build-up is not taken into consideration,

$$P_{fluid}^{max} \approx P_{hyd}\left(1 + 2\frac{\Delta\rho_{boil}}{\rho\beta P_{hyd}}\sqrt{\frac{k_T}{k_{fluid}}}\right) \tag{6}$$

The dimensionless parameter ***Ve*** was defined to enable the quantification of the proximity of this pressure build-up to venting and the following was obtained:

$$Ve = \frac{P_{fluid}^{max} - P_{hyd}}{P_{hyd}} \approx 2\frac{\Delta\rho_{boil}}{\rho\beta P_{hyd}}\sqrt{\frac{k_T}{k_{fluid}}} \tag{7}$$

Considering $\Delta\rho_{boil} \approx \rho/2$, *Ve* can be expressed as follows:

$$Ve = \frac{1}{\beta P_{hyd}} \sqrt{\frac{k_T}{k_{fluid}}} \approx \frac{1}{10^7 Z} \sqrt{\frac{\mu_{fluid} k_T}{k\beta}} \approx \frac{10^{-7}}{Z\sqrt{k}} \quad (8)$$

Z express the intrusion depth in km. If ***Ve*** << 1 the rate of pressure production is slow compared to pressure diffusion. This is due to the importance of permeability of the environment in which a sill occurred. If ***Ve*** >> 1, the sill is emplaced at shallow depths, there is fluid pressure build-up; when the fluid pressure becomes larger than the lithostatic pressure, a 'blow-out' occurs. The overlying rocks are deformed and hydrothermal vent complexes are generated as a result of permeability creation by overpressure fluids (Fig. 1.3.5).

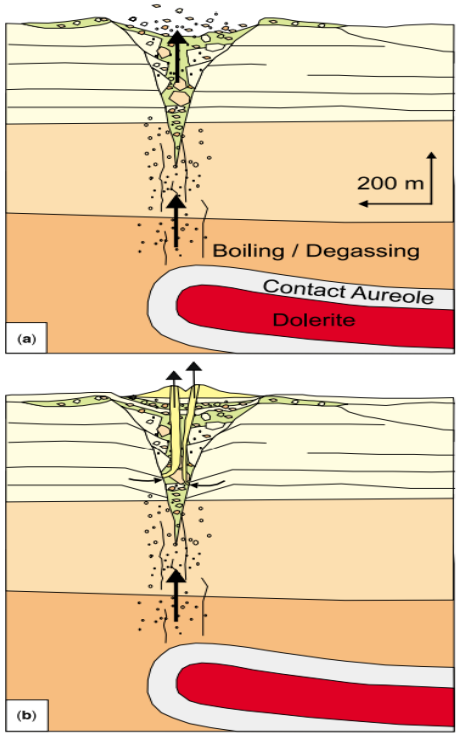

Fig 1.3.4. *Sketch showing the development of a hydrothermal vent complex. (a) Boiling of pore fluids or gas formation (degassing of magma, metamorphic reactions) cause fluid pressure build-up and explosive formation of a cone-shaped hydrothermal vent complex. The initial fluid expulsion is associated with fragmentation and generation of hydrothermal breccias. (b) Subsequently, large (several metres across) pipes of fluidized sandstone cross-cut the brecciated rocks. Smaller hydrothermal pipes (cm-size) form during later reworking of the cone structure, following a reduction in fluid pressure gradients (from Jamtveit et al. 2004*).

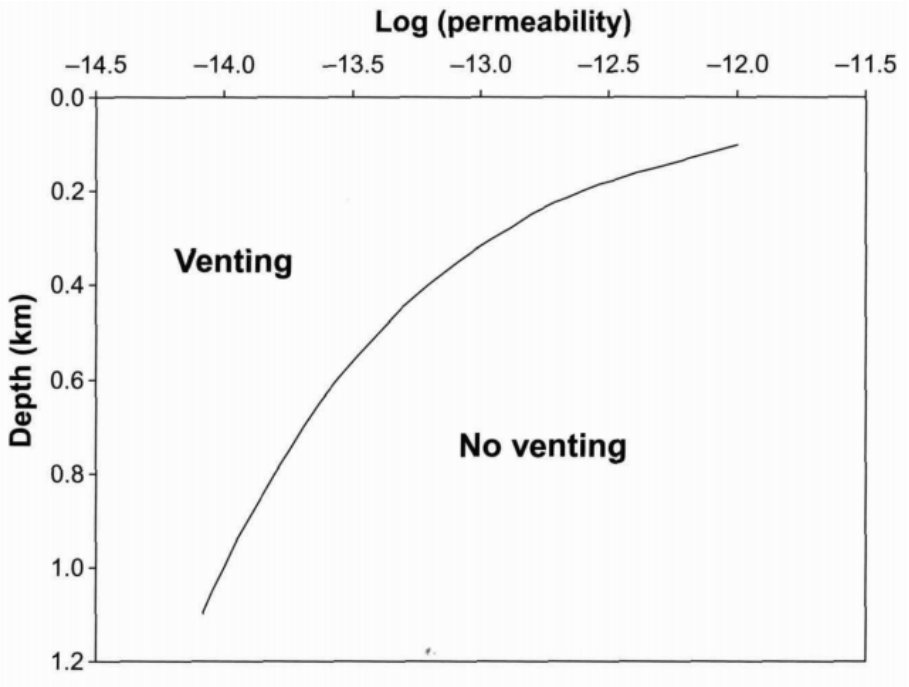

Figure 1.3.5. *Depth of intrusion versus log permeability of country rock for a Ve-value of 1, based on equation (8). Venting may occur in the region where depths are shallow and lor permeabilities are low. In the region to the right, fluid pressure will leak off too rapidly for venting to occur. At depths exceedingc. 1.1 km, boilingdoes not occur in pure water because the lithostatic pressure exceeds the critical pressure. Hence, no venting is expected (Jamtveit et al., 2004*).

2. Study area

2.1 Structural geological settting

Norwegian sea region comprises most of the continental margin between 62^{o} and 69^{o} 30’ N. This part of the Norwegian margin can be described as a rifted passive continental margin. The tectonic development of the Norwegian Sea was more closely influenced by the break-up and formation of the North Atlantic in the tertiary than other parts of the Norwegian Continental Shelf. Both the Caledonian orogeny and break-up of North Atlantic account as the two major plate tectonic episodes that underwent and divide the tectonic history of the Norwegian sea continental margin in the three following periods (Blystad et al. 1995): (1) The pre-Late Devonian, a period ended with the final closure of the proto-Atlantic (Iapetus ocean) during the Caledonian-orogeny in Late Silurian and Early Devonian. (2) The Late Devonian to Paleocene epoch which was characterized by episodic extensional deformation culminating with the continental separation between Eurasia and Greenland at the Paleocene-Eocene boundary. (3) The Earliest Eocene to present epoch characterized by active seafloor spreading between Eurasia and Greenland.

The regional stress regimes also were highly affected by the Caledonian Orogeny and the continental breakup (Blystad et al. 1995). The stress regime that underwent the lithospheric plates before the Late Devonian was compressional before changing into extensional from the Late Devonian until the continental separation in Eocene (Blystad et al. 1995). The stress regime became weakly compressional during the subsequent Tertiary sea-floor spreading (Blystad et al. 1995)

In Middle to Late Devonian time intramontane extensional basins such as Hormelen Basin in onshore Western Norway and the Devonian sedimentary rocks on Ørlandet, Hitra and Fosna formed as a result of orogeny collapse after the Caledonian Orogeny (Blystad et al. 1995).

Considerable rifting episodes affected the area in the Carboniferous (?) and Early Permian in the Late Jurassic and Early cretaceous and earliest Tertiary (Blystad et al. 1995). Besides the area was affected by several extensional tectonic phases in Triassic, Early Jurassic, Aptian/Albian, post-Cenomenian, Late Creataceous and Palaeocene (Blystad et al. 1995).

During Late Carbonifereous to Early Permian, the tectonic activity is characterized by the formation of basins such as Froan Basin and similar others along with a block-faulted terrain (mappable beneath the Trøndelag Platform and the Halten Terrace) with the same age and NNE strike.

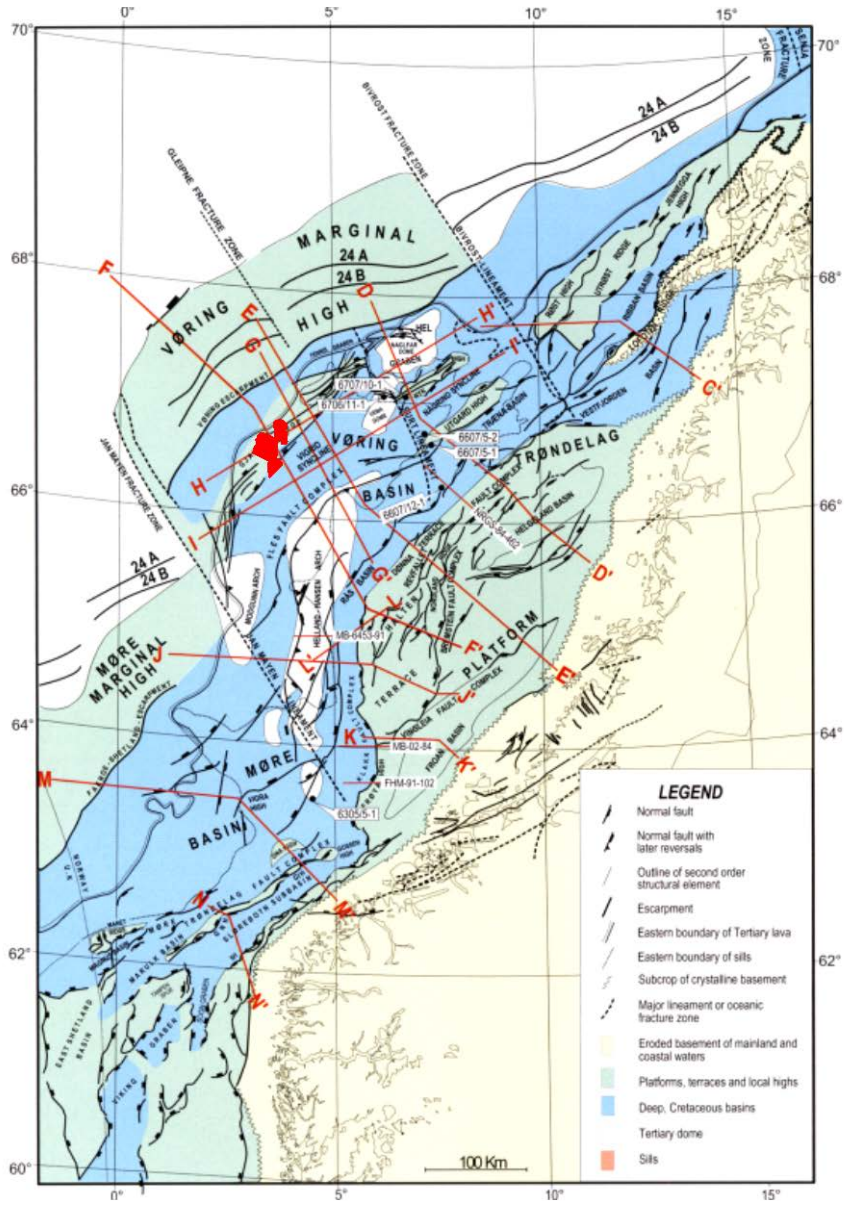

Figure 2.1. Simplified structural map of the Norwegian Sea continental margin (Brekke 2000). Study area in red box.

The development of the basin formed in Permian continued in the eastern part of the Nordland Ridge and Frøya High in Middle to Late Triassic as some block faulting were taking place. Two Triassic evaporite intervals may be mapped in these basins. The halite thicknesses may reach 400m in some places to anhydrites elsewhere. The upper evaporites are dated Carnian meanwhile the lower ones are of Ladinian age (Jacobsen & van Veen 1984). The later rifting episode and subsequent episodes of normal faulting were considered as a period the two evaporites act as important detachment levels for normal faulting (Withjack et al. 1989).

Growth faults trending NNE, probably detached from Triassic evaporites, are observed in Sinemurian/Pliensbachian a period following the Late Triassic and earliest Jurassic, a period characterized by tectonic quiescence (Blystad et al. 1995).

Fangst Group sediments deposition occurred mostly as “blanket sands” during a quiet episode through Aalenian, Bajocian and most of Bathonian times while the Tofte Formation sand deposition preceded the Early Jurassic growth faulting (Blystad et al. 1995).

A very intense rifting episode that can be subdivided into three phases occurred in late Middle Jurassic-Early Cretaceous (Blystad et al. 1995). The western parts of the Trøndelag platform were constituted by the Halten and Dønna terraces during the first two phases that were tectonically most active and that respectively occurred in Bathonian/Callovian and Kimeridgian (Blystad et al. 1995). In addition, faulting and flexuring appeared along the eastern flanks of the Møre and Træna Basins (Blystad et al. 1995). The third phase that occurred in Neocomian, was a period characterized by further development of the basin margins and enhancement of the separation between the platform and the terraces (Blystad et al. 1995).

Remnants of pre-Jurassic basins of unknown history and age are present in the Lofoten-Vestfjorden area after the seismic data (Blystad et al. 1995). The initiation of the basement horsts and the prominent grabens of the area happened in the Jurassic but the development occurred in the Early Cretaceous. The basement is involved by the large-scale faulting and flexuring whereas shallow listric fault detaching into the Triassic evaporites are involved by the smaller-scale tectonics on the Trøndelag Platform and especially on the Halten and Dønna Terraces (Blystad et al. 1995).

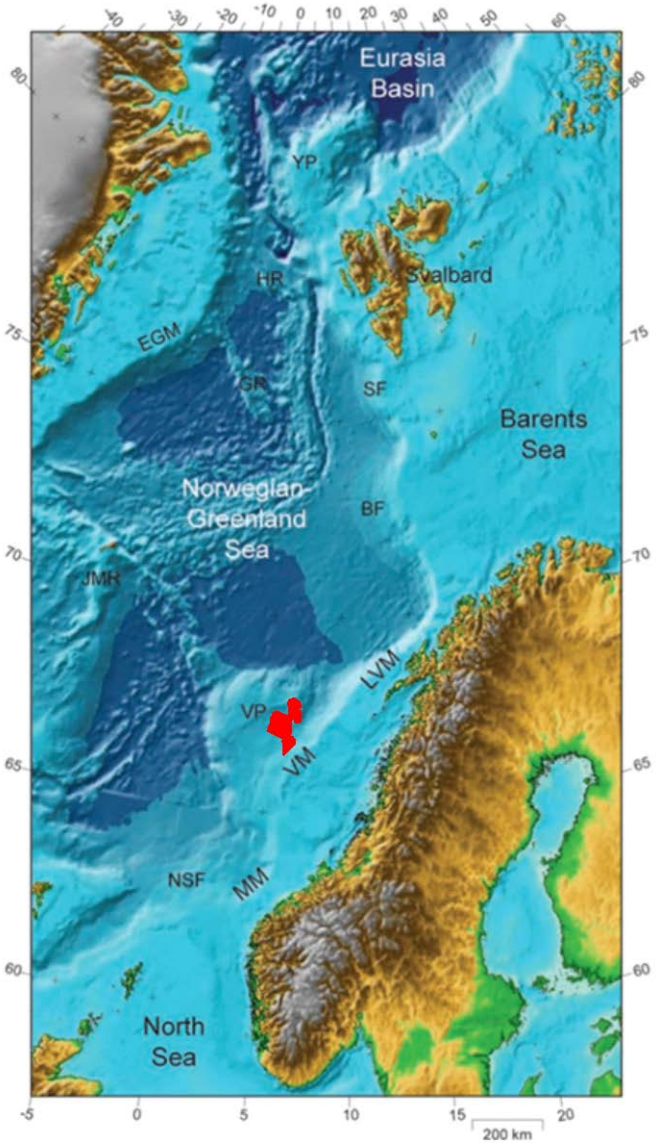

*Figure 2.2 Regional setting of the Norwegian continental margin, which formed in response to the Cenozoic opening of the Norwegian-Greenland Sea. Bathymetry/topography from the 1× 1' elevation grid of Jakobsson et al. (2000). BF: Bjørnøya Fan, EGM: East Greenland Margin, GR: Greenland Ridge, HR: Hovgård Ridge, JMR: Jan Mayen Ridge, LVM: Lofoten-Vesterålen Margin, MM: Møre Margin, NSF: North Sea Fan, SF: Storfjorden Fan, VM: Vøring Margin, VP: Vøring Plateau, YP: Yermak Plateau (Faleide et al., 2008).*The study area in red color.

The second rifting phase was characterized by the uplift and deep erosion of the western edges of the Halten Terrace (the Sklinna Ridge) and the Trøndelag Platform (the Frøya High and Nordland Ridge) (Blystad et al. 1995).

The Vøring and Møre basins underwent principally thermal subsidence during the Neocomean rifting phase and the end of the Cenomanian time. Though important faulting activity along the boundary faults in Aptian/Albian are indicated by the marked expansion of Lower Cretaceous strata in the Ribban, Rås and Træna Basins (Blystad et al. 1995). The reactivation of the

Ylvingen Fault Zone occurred during this period both by normal dip-slip extension and possibly with oblique dextral component (Lokna 1993).

The north of Jan Mayen Lineament shows an evidence for the onset of an episode of tectonic activity at the end of the Cenomanian/Early Turonian Blystad et al. 1995). The uplift and eastward tilting of the westernmost parts of the Vøring Basin triggered the beginning of the Gjallar Ridge formation. In addittion the post-Cenomanian onlapped onto the eastward-sloping upper surface of the Cenomanian along the Gjallar Ridge as a result of uplift and eastward tilting of the westernmost parts of the Vøring Basin (Blystad et al. 1995).

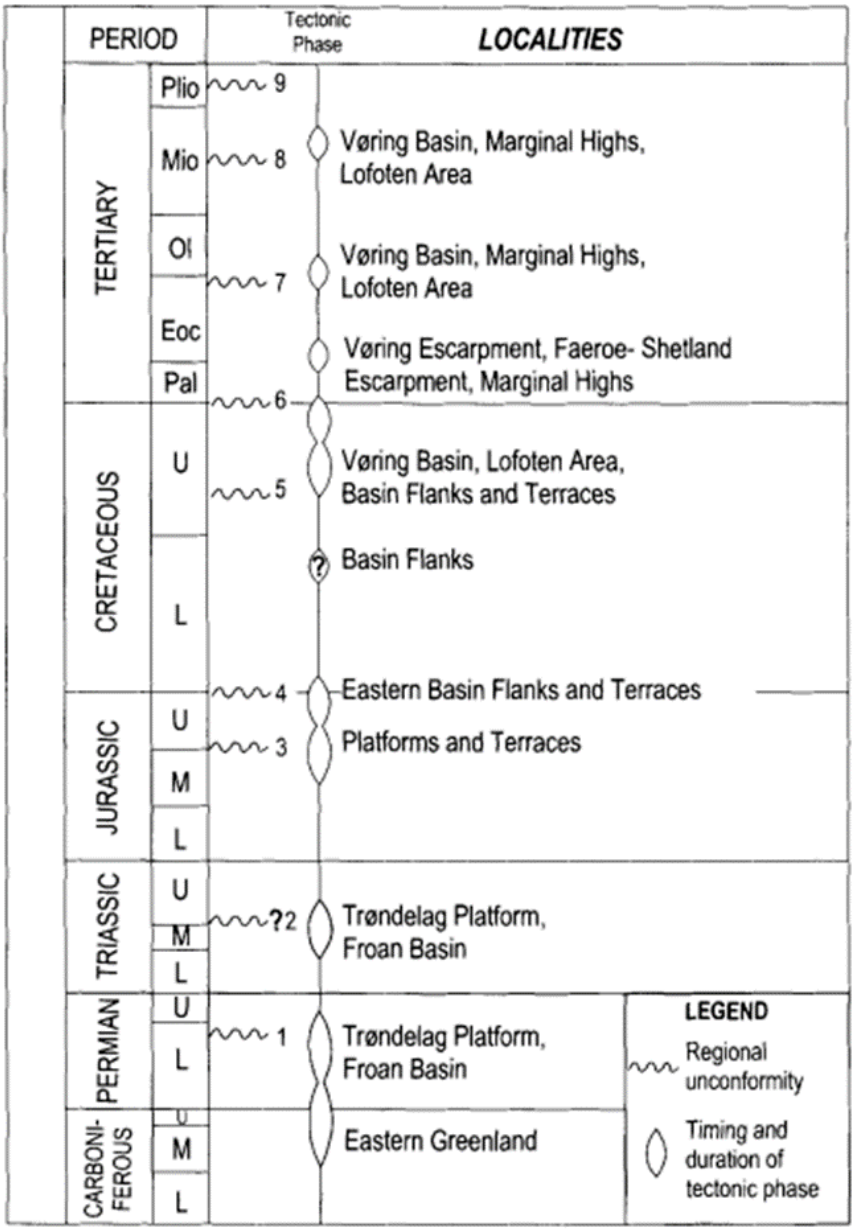

Figure 2.3. *Tectonic history of the Norwegian Sea continental margin (Brekke 2000).*

Volcanic Margins and marginal highs

Numerous continental margins that have been found to have a marginal high and a volcanic overprint around the world (Hinz 1981, White and McKenzie 1989) have been termed volcanic margins (Blystad et al., 1995). The formation of mid-Norwegian margin includes the tectono-magmatic evolution as follows (Eldholm et al., 2002): (1) Plate breakup and separation as a result of lithospheric extension during a rift episode in the latest Cretaceous-Paleocene, (2) central rift uplift and increased igneous activity during late rifting and a few million years after breakup, culminating with voluminous outpourings of basaltic lavas in the early Eocene, and (3) change to normal accretionary magma volumes with subsequent continental margin subsidence and maturation (Middle Eocene-Present).

The volcanic margins off Norway (Figure 1&2) comprising the Møre, Vøring and Lofoten-Vesterålen margins, are generally subdivided into three zones I-III (Figure 4), having different acoustic basement characters (Hinz et al., 1982; Talwani et al., 1983). To the west these zones are bounded by normal oceanic crust. Zone I represents a flow/sill complex east of the Faroe-Shetland and Vøring escarpments. Zone II lies west of these escarpments and is characterized by an almost flat-lying, smooth and shallow volcanic surface under a thin Cenozoic sediment cover. Zone III has a smooth, shallow volcanic surface, like zone II but is underlain by a thick wedge of westward-dipping reflectors. A broad, low-frequency, high-amplitude basal wedge reflector (reflector K in Hinz et al., 1982) is found under eastern parts of this zone, also extending eastwards beneath Zone II. The western part of Zone III is normally associated with oldest magnetic sea-floor spreading anomalies (24B, 24A, 23).

Zones II and III are much elevated with respect to the adjacent ‘normal’ oceanic crust as well as the sedimentary basins to east. Structurally the two zones therefore form a ‘marginal highs’. The present understanding of these highs is closely linked to advances made in the understanding of passive margins in general.

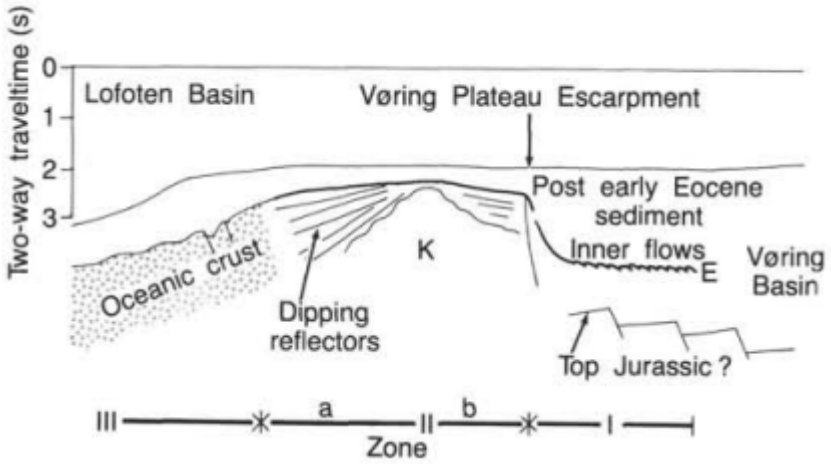

Figure 2.4. Schematic geological section across Vøring Plateau Escarpment. Zone III shows normal oceanic crust. Zone II shows sub-basalt reflections (a: dipping, b: horizontal or subhorizontal). Zone I shows inner flows (Eldholm et., 1984).

Structural elements of the study area

Vøring Basin

The Vøring Basin was defined by Åm (1970) and then by Rønnevik et al. (1975). This basin is located between 64 º N- 68 º N and 2 º E- 10 º E and consists of grabens, basins and structural highs (Blystad et al. 1995). This structural element is bounded in the north and south by the Brivost and Jan Mayen Lineaments, respectively (Blystad et al. 1995). The Vørin Basin is bounded in the east by the Kristiansund-Bodø Fault Complex and the basement highs forming the extension of the Lofoten trend (Figure1)(Bukovics & Ziegler, 1985). The Vøring basin is bounded in the west and northwest by the Vøring Plateau Escarpement (Figures 1&2)(Bukovics et Ziegler, 1985).

The formation of the Vøring Basin occurred during and subsequent to a major Late Jurassic-Early Cretaceous extensional episode (Skogseid et al. 1992b). The Surt Lineament which is parallel to the Jan Mayen and Brivost Lineaments divides the basin as follows (Blystad et al. 1995): a central anticline occurring in the Vøring Basin in the Cretaceous along the Fles Fault Complex is flanked by two synclines, south of the Surt Lineament; the basin is divided into three synclines in the north of the Surt Lineament into Træna Basin (east), Någrind Syncline and Hel Graben (west) separated by the Utgard and Nyk Highs.

Gjallar Ridge

The Gjallar Ridge is named after the bridge of Gjallar described in the Norse mythology. This structural high is part of the Smøla Rift (Rønnevik et al. 1983). The Gjallar Ridge and the Fenris Graben are the two structural elements that composed the Smøla Rift (Bukovics et. 1984). As

part of the Voring Basin, the Gjallar Ridge comprises deeply eroded and rotated fault blocks trending between 65^{o} 30'N-67^{o}30'N and 3^{o}E-6^{o}E (Blystad et al. 1995). These faults principally involve the pre-Tertiary sequences and have a westward polarity (Blystad et al. 1995). The Vigrid syncline bound the ridge to the east whereas the western part is partly hidden beneath Eocene lava flows, except in the north where faults bound it along the Fenris Graben (blystad et al. 1995). The Gjallar Ridge ends at the Rym Fault Zone in the Surt Lineament to the north, and it stops against the Jan Mayen Fracture Zone to the south.

2.2 Lithostratigraphy

Since the discovery of oil and gas in the Norwegian continental margins numerous commercial wells have been drilled and industrial 2D and 3D seismic data were acquired by oil and gas companies and research institutions. This scientific inquiry resulted in better understanding of the basins and the geology of the area. The lithostratigraphy accounts amongst the valuable scientific achievements of this work coordinated by the Norwegian Petroleum Directorate (NPD). Previous studies in the area were performed by the utilization of some of the surveys involved in the present study. The well 6704/12-1 tied to the seismic survey SG99604 enable to date the stratigraphic successions. The stratigraphy provided by the well was correlated with seismic using sonic-log data. The Cenozoic successions have been identified through seismic reflectors.

2.2.1 Rogaland Group

The Rogaland Group, named by Deegan and Scull (1977), comprises Paleocene rocks made up of claystone with minor interbeds of sandstone near the Norwegian margin (Dalland *et al.*, 1988). Marls and reworked limestones are frequent amongst the basal deposits. In the upper part the shales are more and more tuffaceous. The sediments were deposited in a deep marine environment in the Nowegian sea. This group is dated Danian to Late Paleocene in the Norwegian sea and overlain by the Hordaland Group (Deegan et Scull, 1977; Dalland *et al.*, 1988).

2.2.2 Hordaland Group

The Hordaland Group (Deegan & Scull, 1977) consists of claystones and bio-siliceous ooze in the large part of the Oligocene-Miocene sequence of the western Vøring Basin (Dalland *et al.*, 1988; Hjelstuen *et al.*, 1997). The Brygge formation (Fig 4.1) is principally made up of claystones with biogenic ooze and interbedded by sandstones. The Hordaland Group sediments were deposited in marine environment during Early Eocene to Early Miocene and overlain by the Nordland Group (Dalland *et al.*, 1988).

2.2.3 Nordland Group

Named by Deegan and Scull (1977), the Nordland Group is subdivided into the Lower Miocene to Upper Pliocene Kai Formation (Dalland *et al.,* 1988) and the Upper Pliocene Naust Formation (Dalland *et al.,* 1988). The uppermost part of the Kai formation does not occur in the Vøring Basin. The ODP well 642B shows a depositional hiatus separating the overlying Naust Formation and the preserved part of the Kai formation occurred between 3.1 Ma and 2.5 Ma (Jansen and Sjøholm, 1991).The compressional phase that occurred from the end of Middle to Upper Miocene resulted in period of transgression unfavorable to sediment deposition (Eidvin *et al.*,2000; Løseth and Henricksen, 2005). The hiatus may also be caused by the erosion of the upper Kai Formation which is common in the Norwegian margin (Eidvin *et al.,* 2000) as a result of regression between 4.2 Ma and 2.8 Ma (Vail and Hardenbol, 1979). The lithology consists of alternating claystone, siltstone, sandstone with limestone interbeds and widespread pyrite, glauconite and shell fragments in Kai Formation and deposited in a marine environment with varying water depth during early Miocene to Late Pliocene time. The Naust Formation is characterized by interbedded claystone, siltstone and sand, with very coarse grains at irregular intervals in the upper part deposited in a marine environment in Late Pliocene. The Nordland Group extends from Early Miocene to Recent (Dalland *et al.*, 1988).

3. DATA AND METHOD

3.1 Data

3.1.1 Seismic data

Five seismic datasets were used in this study (Figures 3.1,2). The SG604 were acquired by SAGA Petroleum. The bin size (inline/cross line spacing) of the interpreted data is 18.75m x 18.75 m. the dominant frequency is ranging from 40 to 50 Hz and an inline and crossline spacingof 56. The dominant frequency is in order of 30-50 which is also the horizontal resolution. The vertical seismic resolution will therefore be of the order of 10 m given that value should be a quarter of the wavelength (Hansen *et al.*, 2005).

3.1.2 Well data

3.1.2 Well 6605/1-1

This well was drilled in the Vigrid Syncline of the Vøring Basin in the Norwegian Sea. The primary objective of the well was to prove hydrocarbons within a deep marine turbidite system. The principal target was two sand lobes fromMaastrichtian age, within the Springar Formation. The secondary objective was to evaluate the Late Cretaceous Nise Formation. Other objectives in the main reservoir section were to verify the Springar reservoir properties and calibrate the Springar section to the seismic. The well was permanently abandoned in 2009 as dry well (NPD).

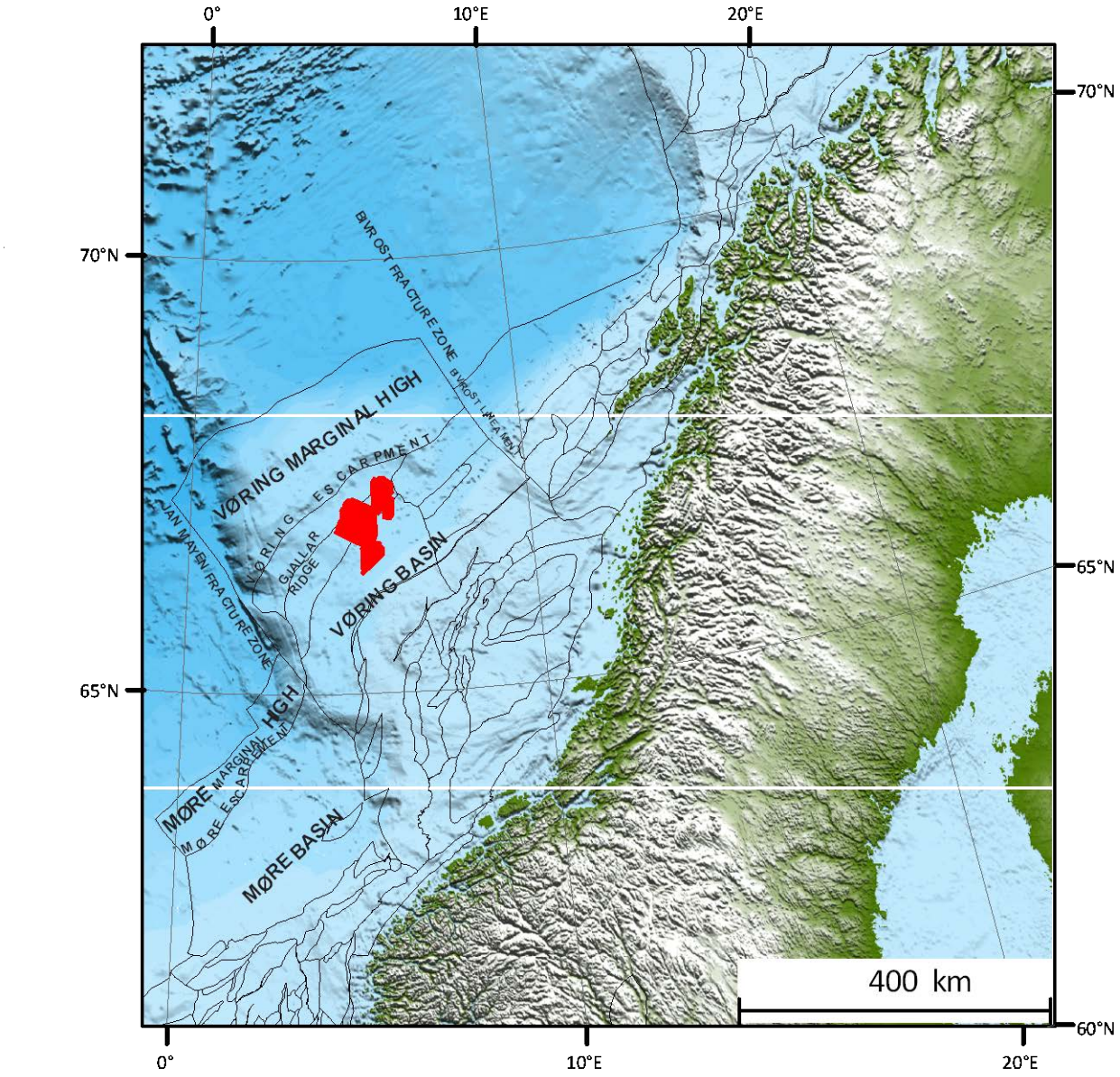

Figure 3.1 Bathymetric showing the location of the study area in red polygon.

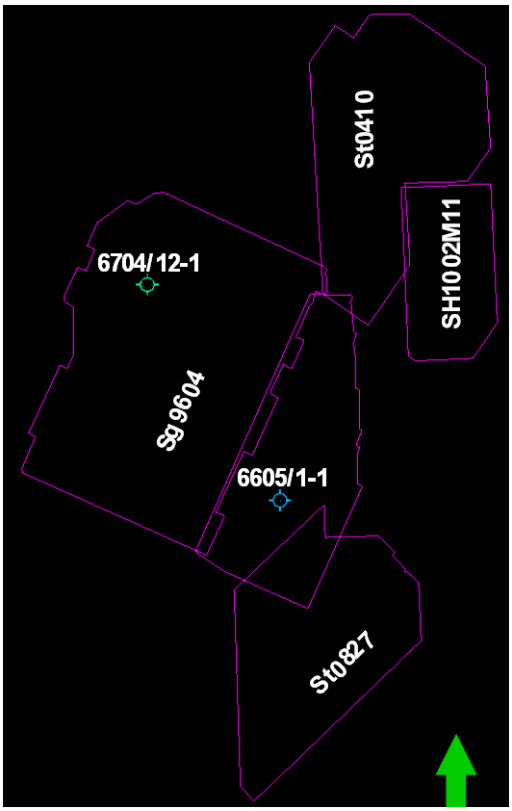

Figure 3.2 Map showing well locations with respect to the dataset (See figure 3.1 for location).

3.1.3 Well 6704/12-1

The well is located on the Gjallar Ridge, on a local horst within a major top Cretaceous four-way dip closure. The main purpose of well 6704/12-1 was to test the petroleum potential of the Upper Cretaceous section. In addition to the primary objective, the well was designed to test the petroleum potential of the possible sandy Eocene section above the main target. The well was permanently plugged and abandoned as a dry hole on 24 July 1999 (NPD, 2003).

3.2 Method

The 3D seismic data were analyzed using Schlumberger's Petrel seismic- to – simulation software (version 2013) for seismic interpretation of numerous horizons in the dataset. The detailed work includes the identification and visualization of vent complexes by means of time and horizon slices using a variety of seismic attribute generated from interpreted seismic horizons and displayed in both 2D and 3D windows. The sill complexes needed to be identified and mapped.

3.2.1 Horizon interpretation

There are several different ways to do horizon interpretation in Petrel: (1) Manual interpretation allows the user to click on key picks and then an interpolation is done linearly between these picks. (2) Autotracking tool is subdivided in (i) seeded 3D autotracking, this method could not

be used due to the poor quality of the reflectors, here points are tracked outwards from the seed points in all directions. (ii) seeded 2D autotracking, points are tracked in the direction of the active (inline or crossline) intersection and will continue until it does not fulfill the constraints specified in the autotracking tab; (iii) guided autotracking, after the selection of two points, the tracking finds the best route from one to another; this option was used given that it gives a high degree of control as to how the interpretation will develop; (iv) paintbrush autotracking, it works only in 2D windows, it was used after an interpretation of several inlines and crosslines in order to have a clean horizon. (v) active box autotracking, it also works only in 2D windows, here the user drags a rubber band, capturing some seed points within its area; upon releasing the rubber band, autotracking occurs inside the active box area.

Parameters' setting is important before starting any horizon interpretation. For instance the seed confidence for a 3D cube needs to be specified, which event to track (z-crossing, peak, trough or s-crossing) has to be chosen in the tracking mode.

3.2.2 Seismic attributes

3.2.2.1 RMS attribute

RMS Amplitude is the square root of the squared amplitudes, divided by the number of live samples as shown in the following formula:

$$[(\Sigma i^{n}\ amp^{2})/k]^{1/2}$$

Where k is the number of life samples.RMS may directly to hydrocarbon indications in the data and other geologic features which are isolated from background features by amplitude response.

3.2.2.2 Variance

Variance is used to extract an edge volume from an input seismic volume.

3.2.2.1 Thickness Mapping

Thickness of stratigraphic units provides information such as syndepositional structural development and depositional trends to name but a few. The isochron maps were used in this study to evaluate the thickness of formations from seismic. An Isochron map is by definition a contour map of equal value of seismic travel time (Tucker, 1998).

4. RESULTS

4-1 Stratigraphy

The stratigraphy of the study area can be deducted from the identification of the surfaces in the seismic data tied with Well data in one hand and previous studies in the other hand. Other reflectors that can be correlated by the overlapping dataset in other to in order to better understand the stratigraphy of the study area.

Naust formation

The uppermost stratigraphic unit consist of sediment that were deposited as early as the Pleistocene time. The thickness of the sediment is not uniform from one place to another in the study even though the structure occurring in this formation are quite similar after their seismic expressions. This unit represent the Naust formation that is deposited on the regional unconformity that occurred in early Pleistocene. This Base Pleistocene Unconformity (BPU) can be recognized in the study area by its high seismic reflections and its hummocky reflections that occur in datasets. The relief of this surface may be as high as 0.2 s TWT and is mainly affected by polygonal faults. The reflections are generally continuous within the Naust sequenses in study area except in the datasets SH1002M11 and ST0410 where the disturbed reflections are visible.

Kai Formation

The base of Kai formation is characterized by a high density of faults and high amplitude reflections. The datasets exhibit by continuous reflections mainly characterized by low amplitude especially exacerbated between the Opal A/CT reflector and the BPU that limits the kai formation with the overlying Naust formation since the uppermost part of the Pliocene is missing in the Vøring Basin. That regional unconformity (BPU) indicates the onset of glacially dominated deposition (Faleide *et al.*, 1996). Unlike the rest of dataset, the survey ST0827 exhibits a Kai formation characterized by high amplitude reflections.

Brygge Formation

The Brygge formation accounts with the overlying Kai formations the thickest stratigraphic units. The deposition of formation took place during the Eocene and Oligocene time. The intra-Oligocene reflector is characterized by dipping reflections and reliefs that can be up to 100 ms high. The seismic reflections are relatively continuous compared with the underlying Tare formation.

Tare Formation

This stratigraphic unit consists of disturbed seismic reflections. This formation is the first Cenozoic sedimentary unit to be put in place. The sedimentation took place during the Paleocene time over an unconformity.

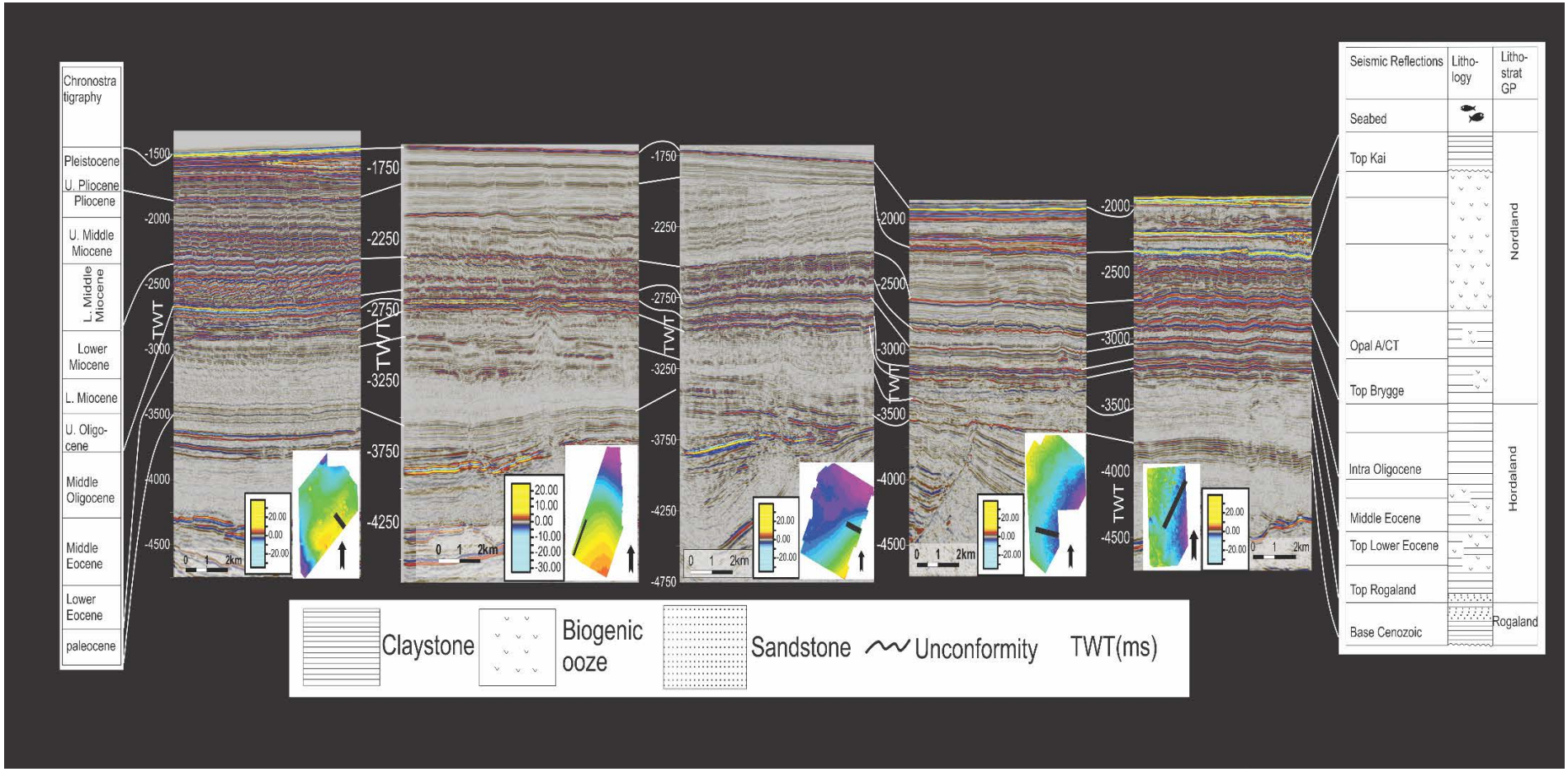
Chronostratigraphy
Pleistocene
U. Pliocene
Pliocene
U. Middle Miocene
L. Middle Miocene
Lower Miocene
L. Miocene
U. Oligocene
Middle Oligocene
Middle Eocene
Lower Eocene
paleocene
TWT
Claystone
Biogenic ooze
Sandstone
Unconformity
TWT(ms)
Seismic Reflections
Litho-logy
Litho-strat GP
Seabed
Top Kai
Opal A/CT
Top Brygge
Intra Oligocene
Middle Eocene
Top Lower Eocene
Top Rogaland
Base Cenozoic
Nordland
Hordaland
Rogaland

Figure 4.1 Seismic sections illustrating the stratigraphic setting of the study area, unconformities, and lithology of the units. BPU: Base Pleistocene Unconformity. The correlation of the seismic reflections and lithostratigraphy are from Hansen et al., (2005).

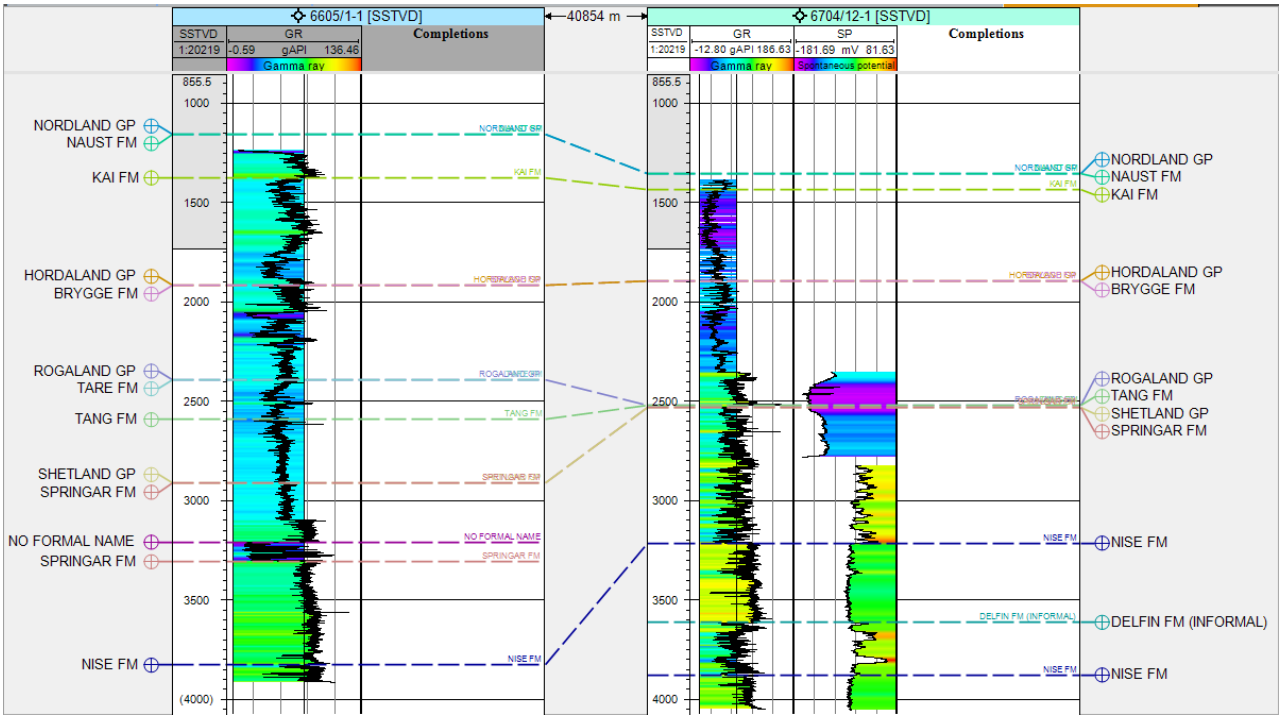

Figure 4.2 Wells 6704/12-1 and 6605/1-1 tied with the dataset showing the correlation between the stratigraphic unit and the sediment properties. GR (gamma-ray).

4-2 Structural interpretation and Volcanic intrusions

The focus of this sub-chapter is on the mapping and interpretation of deformation and volcanic intrusions that have undergone the stratigraphic units throughout the geological timescale.

4-2-1 Distribution of structural deformations in the study area

Faults include of deformation processes that resulted in fracturing and the displacement, be it slight or significant, of the sedimentary formations. The materials affected might include the stratigraphic units beneath the seabed or the seabed itself.

The entire study area exhibits a network of relatively low displacement faults that affect the upper part of Brygge Formation and extend further to the Opal A/CT reflector in the Kai Formation. A variance time slice taken along the upper part of the Brygge Formation shows the polygonal geometry of the faults (Fig.4.3). That map shows that the density of polygonal faults increases westwards. Some fault networks make up a radial geometry as the Figure 4.3 illustrates the deformation is recurrent in the upper part of the Brygge Formation in the western

part of the study area. Normal faults are widespread in the dataset and they extend to the BPU where some of them affect the lower part of the Naust Formation and might even go further to the seabed. However, the western part of the dataset shows a localized network of polygonal faults. Their occurrence between the Opal A/CT and Naust reflections is relatively meaningless compared with that of the faults developed between the top Brygge and Opal A/CT reflectors. However, these shallower faults formed with significant fault planes be exceeding the BPU reflector. In plan view these fault networks appear as interconnected polygons. A variance attribute generated along the base Naust horizon shows some localized polygonal faults in the western part of the study area surface. These faults are bounded by a an area deprived of visible deformation before occurring again at the eastern part of a sub-circular feature and at the southern part of a feature located at the southern part, of these polygonal faults, and the rest of the study area.

A fault network made up of small patterns following a zigzag path occurring in the eastern part of the study area is separated from polygonal faults by a less dense fault network. This fault network appears in both time slice and attribute map generated respectively from upper Brygge seismic reflections and bass Naust reflections. These faults do not exceptionally have a greater extent. This appearance is likely due to the isolation of faults making up the network from the dense polygonal faults seating in the western part. It worth noting some polygonal faults have similar extent as it is shown in seismic section but their significant density in plan view in the western part of the study area makes it difficult to identify or pick and locate polygons at different levels in the time slices or attribute maps. However, the visualization of fault networks in plan view shows the incommensurate distribution of faults between the upper part of the Brygge Formation reflections and the base of the Naust Formation reflections (Fig.4.3). The deeper part as well as the shallow part of the study area shows evidence of brittle deformation. The seismic section exhibits fault blocks and minor faults characterized by a low displacement. Some of the fault planes are characterized by high amplitude reflection occur in the in the Cretaceous. Figure 4.8 displays rotated faults that were found in the center of the study area and bounded by a disturbed stratigraphic unit where sill complexes occur.

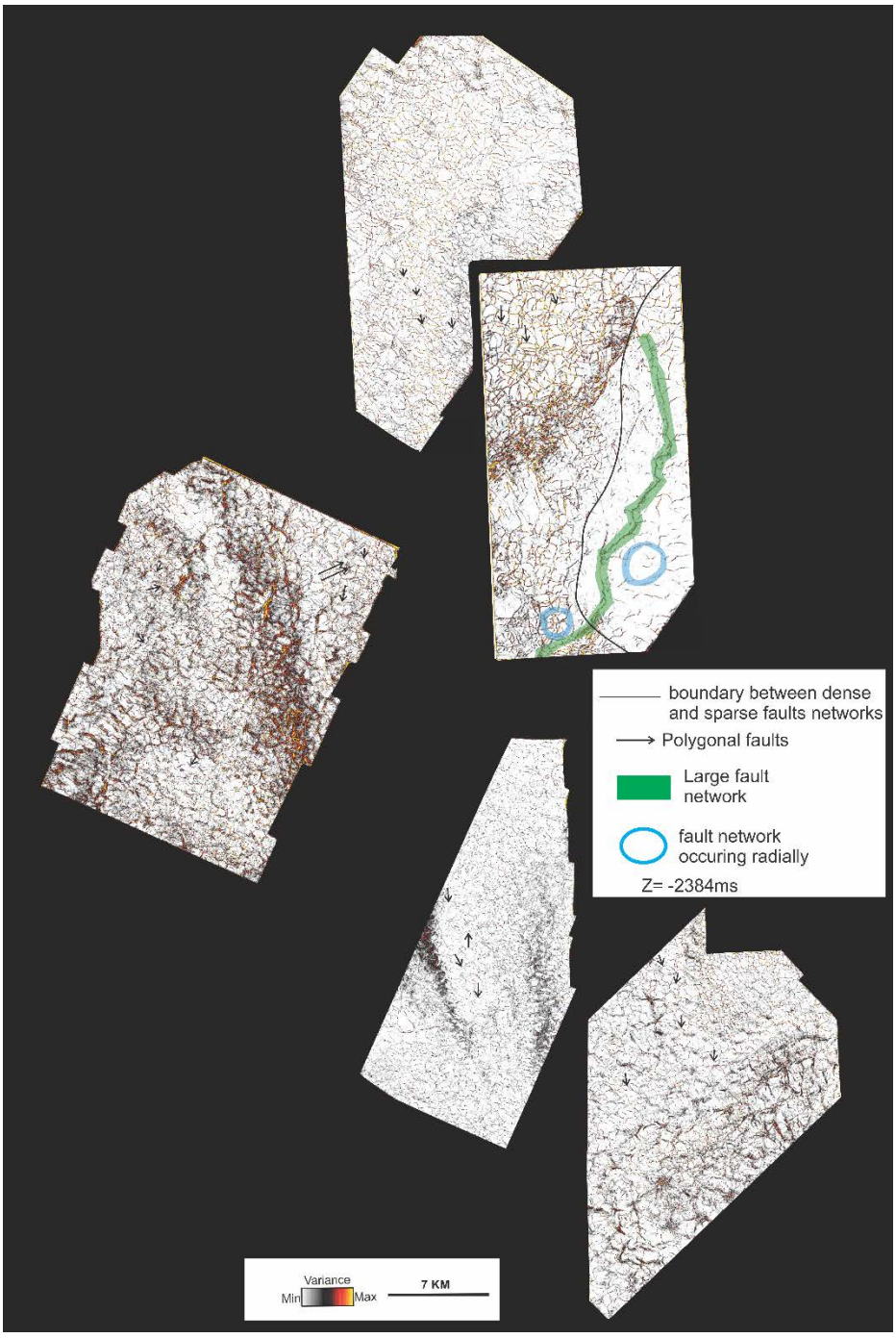

Figure 4.3 Time slice along the Brygge Formation(TWT: -2384) showing the distribution overview of faults in the study area. The polygonal faults are widespread and dense. Some fault networks occurring radially can be identified where the polygonal faults are sparse.

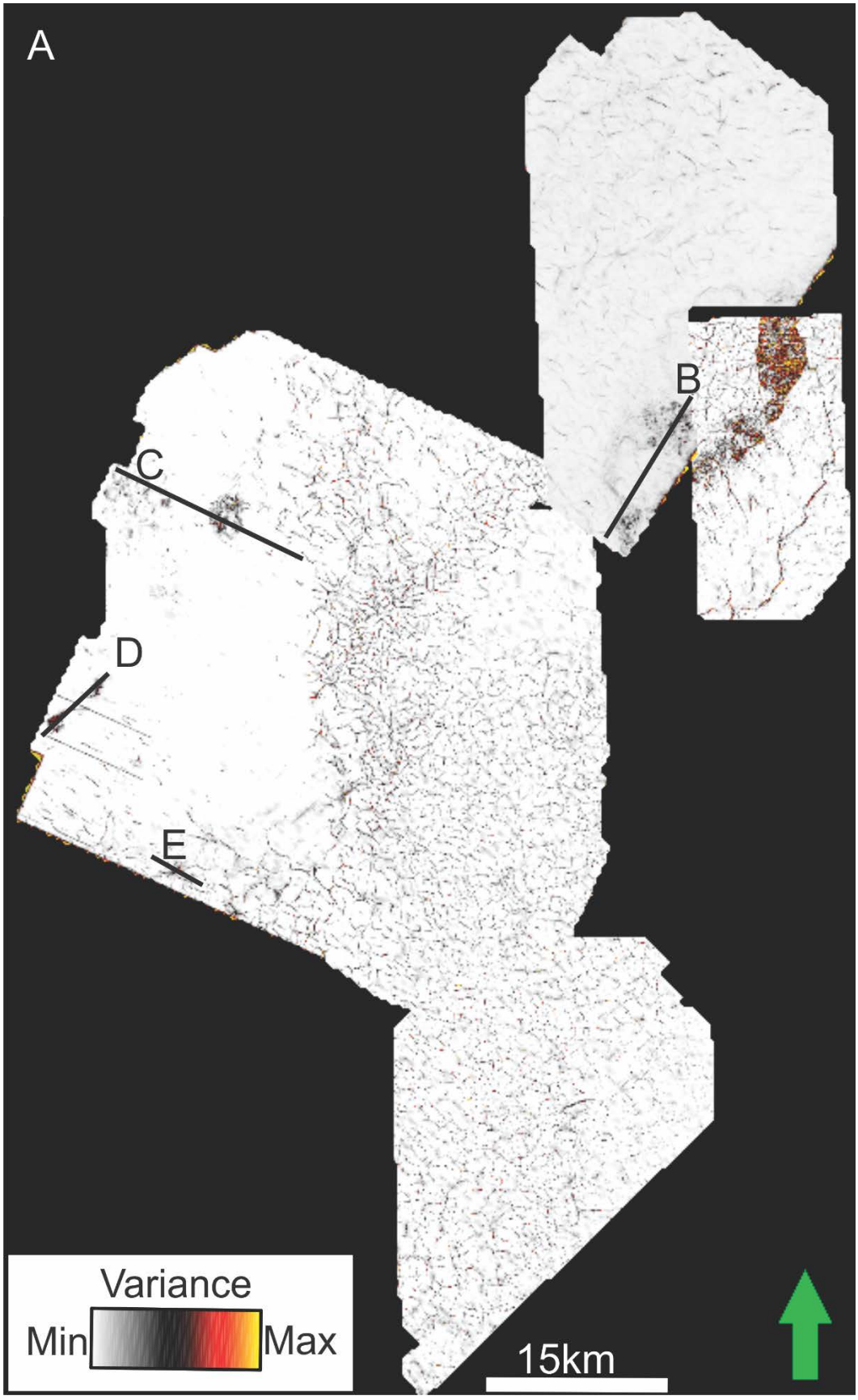

Figure 4.4 A. variance attribute along the base pleistocene unconformity (BPU) showing a spatial distribution of faults. B, C, D, E represent seismic sections across BPU.

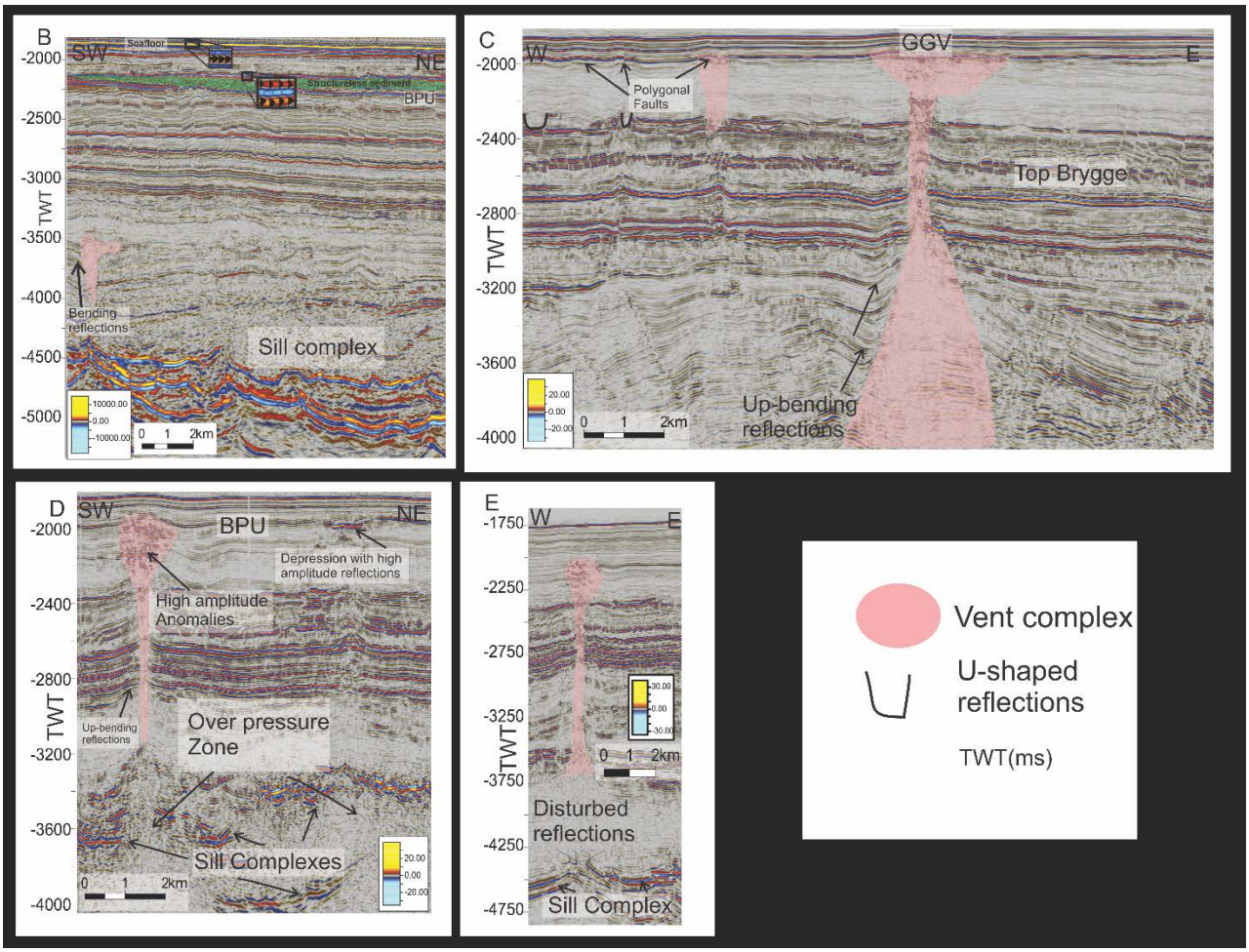

Figure 4.5 Seismic sections across the dataset showing in **B**) the structureless sediment seating above the BPU, reversal phase of the reflections with respect to that of the seafloor., sill complexes and hydrothermal vent complex provoking down bending reflections, in **C)** polygonal faulting and vent complexes within the BPU, in **D)** vent complex and high amplitude anomalies associated with, and the sill complexes, in **E)** vent complex associated with high amplitude anomalies.

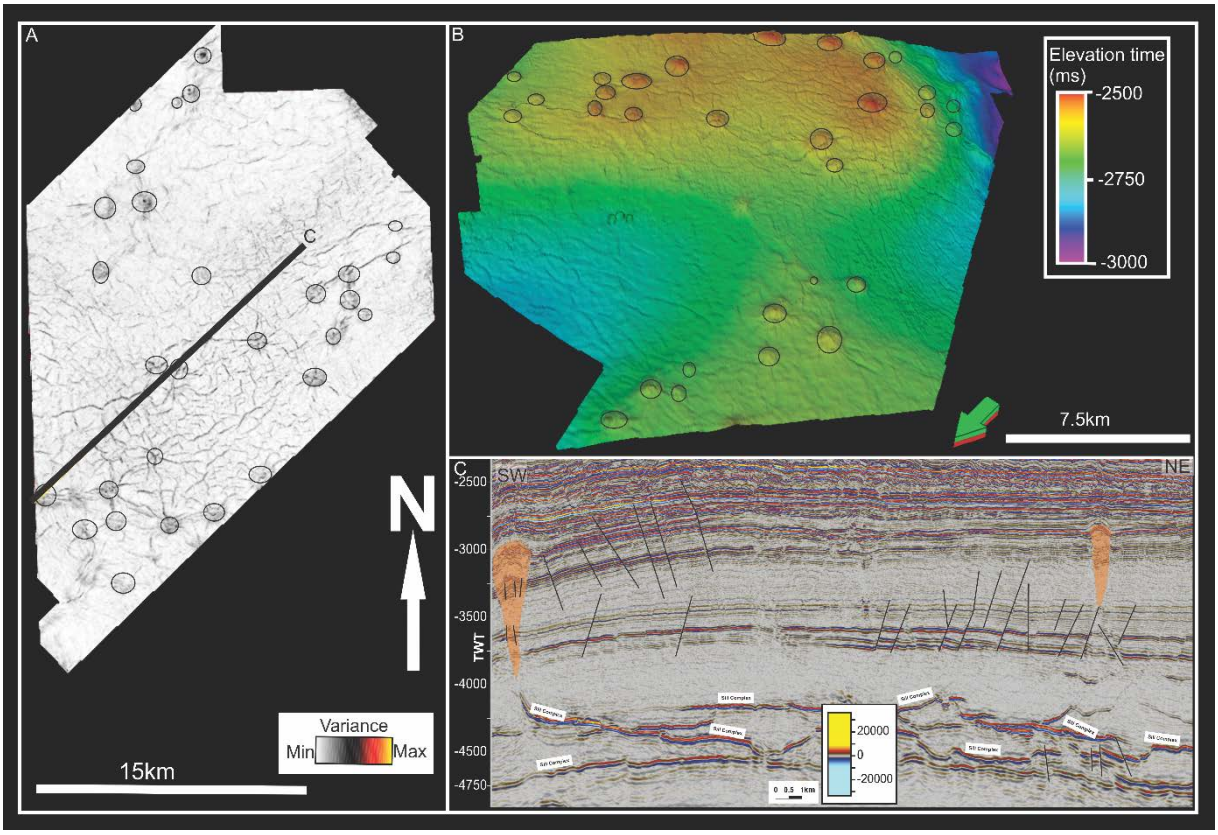

Figure 4.6 variance attribute and time structure map computed along the intra-oligocene horizon showing in **A)** a variance attribute showing spatial distribution of mound structures and their relationship with the faults they are associated with, in **B)** a time structure map showing the mounds that are subtle in variance, the vertical exaggeration is 5, in **C)** a seismic section the mounds and their relationship with faults and sill complex distribution.

The end of faulting in the NGR is prior to the break-up (Early-mid Paleocene). The dataset displays rotated faut blocks

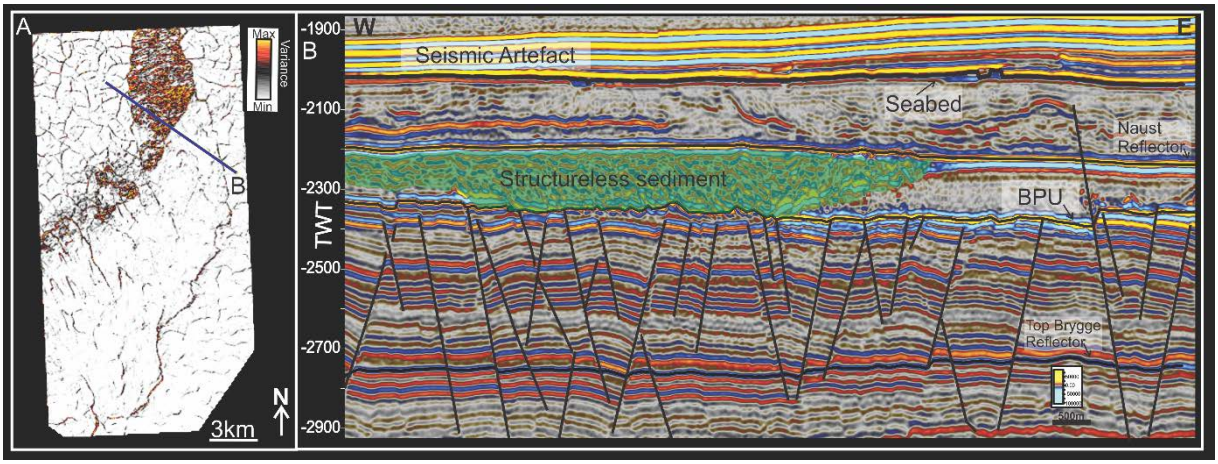

Figure 4.7 Structure distribution showing in **A)** a variance attribute showing a slide scar in the area and fault networks and displayed in seismic section in **B)** seismic section showing normal faults extending to BPU, transparent reflections and a package structureless sediment seating on top of the slide scar occurring in the stratigraphic unit between BPU and Naust reflector.

Folding

Beside the occurrence of faults, the seismic data displays another type of deformation. The morphology of the stratigraphic units change in response to stress. The morphology adopted as a result of deformation is dependent upon the behavior of the material affected. In the study area several reflectors, discrete and continuous, bend up or down. In the large scale the right terminology to characterized the shape taken by rocks include syncline and anticline. Nevertheless, the characteristics are similar i.e the up and down bending of the rock-unit hinge characterizing anticlines and synclines respectively. They are also visible in smaller scale. Hence the dataset exhibits at several locations positive relief. The domes are sometimes fractured or faulted, present high amplitude reflections, or simply play as a barrier to features that are presumably unconsolidated material and/or fluid due to their seismic expression which is high amplitude or chaotic (Fig.4.5).

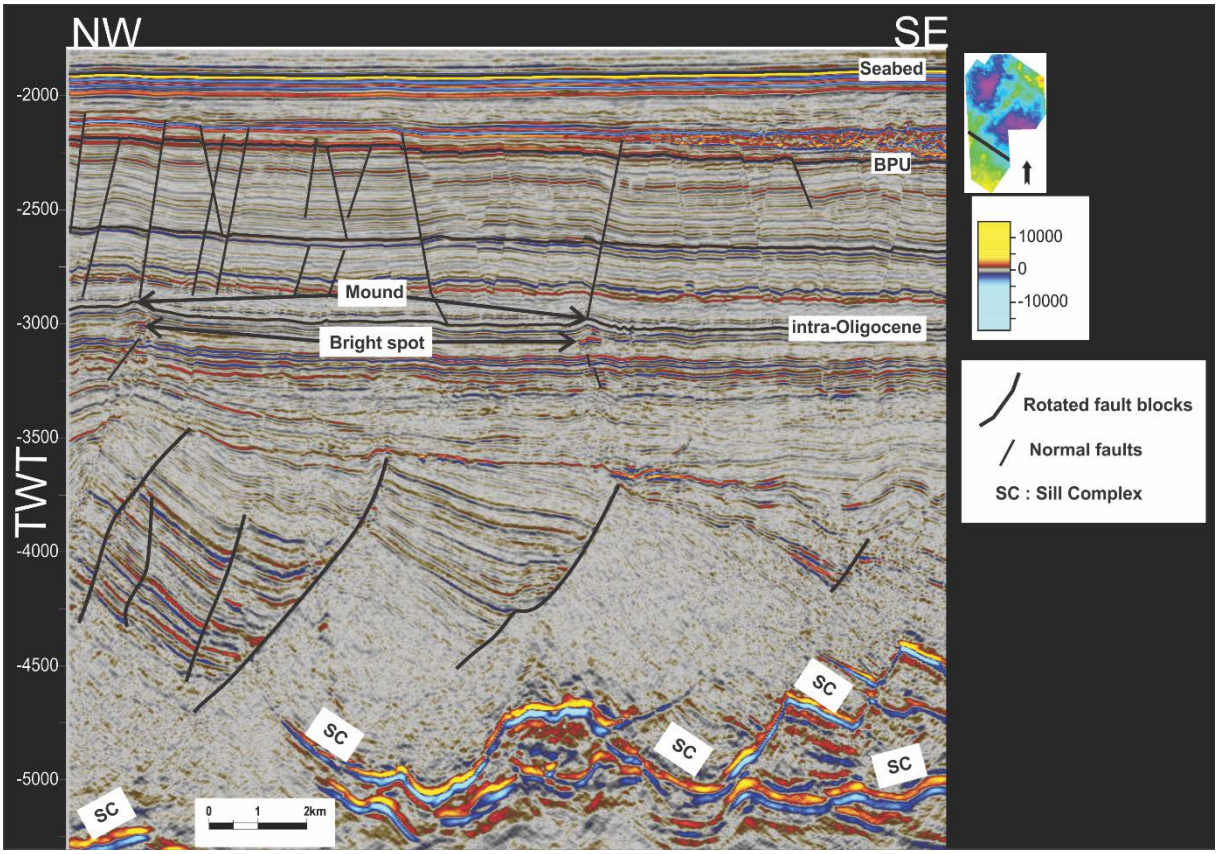

Figure 4.8 Seismic section displaying structural features and volcanic intrusions in the study area.

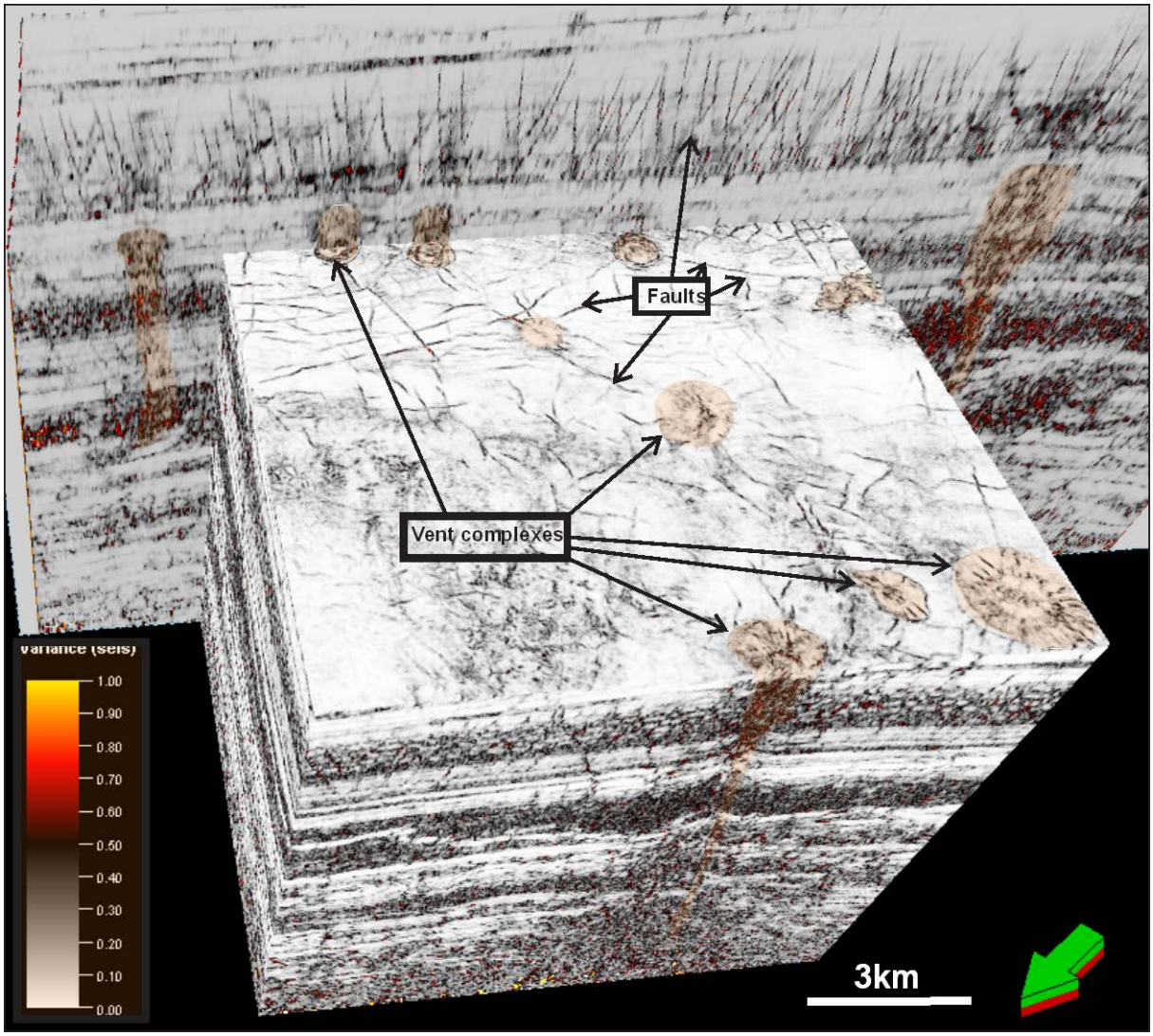

Figure 4.9 Variance cube showing faults and and vent complexes in the dataset.

4-2-2 Volcanic intrusions

The early Eocene sequence displays a variety of features that can be investigated seismically. Unlike the shallower depths, this level is characterized by significant acoustic disturbances. However, distinct features are encrusted in this level. They are recognizable by their seismic signature and particular various shapes. They may occur in group or isolated in a seismically chaotic environment. These features are remarkable by their high amplitude reflections meanwhile their surrounding sedimentary strata arecharacterized by very low seismic amplitude (Fig.4.8 and Fig4.13C).

These features present various facies units as they are introduced into sedimentary formations. They may occur sub-vertically, sub-horizontally or may be mimicking the stratigraphy. They relationship between one feature and its neighbors is visible through seismic profile. This angle

of description shows that the features may appear connected to one another as two rings, or vertically staked. The interpretation followed by a three dimensional view enables an inner structure description of these features and the following morphologies are brought into light.

- Saucer-shaped features, they are widespread in the study area and may occur in group i.e interconnected in step-like structures and emplaced obliquely in the stratigraphy; in seismic section, the feature is characterized by high amplitude reflections and follow a down bending shape with edges terminating at different TWT.

- Canoe-shaped features, they present two axis thus one long and one short sometimes seating on a round concave base or a basal hinge linking the edges of the long axis (Figure 4.10 A).

- Tongue-shape features, these features may occur alone or as a link between two features of different morphologies.

Several sedimentary basins around the world present similar structures that have been interpreted as sills. Both Seismic analysis and Field provided detailed analysis of these features as they occur off shore Mid-Norway in the Møre and Vøring Basins (Sørensen et al., 2004; Planke et al., 2005; Hansen and Cartwright, 2006), on the NW Australian shelf (Symond et al., 1998), in the Faroe-Shetland Basin (Smallwood and Maresh, 2002; Hansen et al., 2004), offshore Scotland in the Rockall Trough (Thomson and Hutton, 2004), offshore Senegal (Rocchi et al., 2007; Hansen et al., in press), and in the Karoo Basin (Chevalllier and Woodford, 1999). Planke et al. (2005) subdivided sill facies in group comprising their possible configuration as they are encountered in the Vøring and Møre basins.

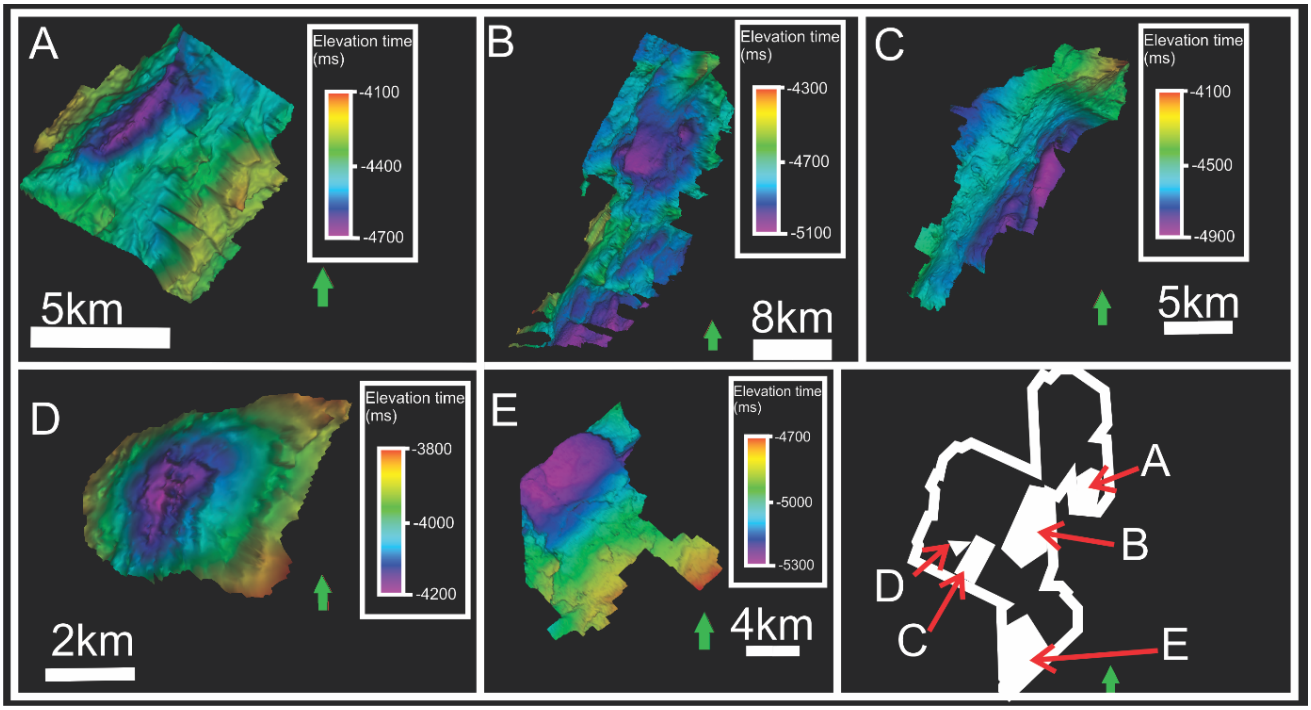

Figure 4.10A-E sill complex shape canoe-shaped sill complex, **A)** canoe-shaped sill complex, **B)** Layer parallel with slightly convex sill, **C)** Tongue-shaped sill complex, **D)** Saucer-shaped, **E)** Semi Saucer and layer parallel sill complex.

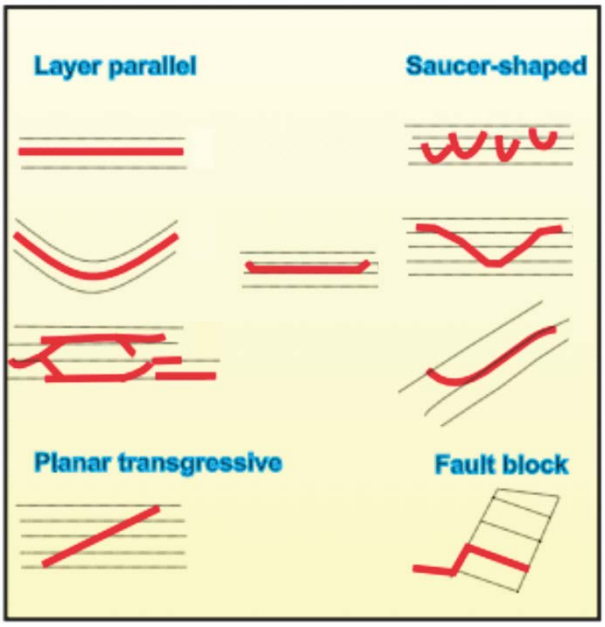

Figure 4.11 *Sketch showing the configuration of identified sill facies units* (Planke *et al.*, 2005).

4-3 Interpretation of fluid flow features

4-3-1 Description and Interpretation of Mounds and pipes

This sub-chapter provides a description and interpretation of vertical features occurring in the dataset. The investigations will be carried out all the way from the mappable deepest horizon

to the seabed where fluid flowing through the sedimentary successions might be seeping in the seabed if the migration is not prevented either by structural architectures including faults, or overburden formed by sealing lithology rocks therefore those the rocks characterized by low permeability and high density. These features rise upwards like a column from early Eocene and terminate at different level in the Cenozoic. The results will be quantitatively and qualitatively presented with respect to the features appearances and occurrences in the stratigraphy within the seismic data.

4-3-2 Mound features

The mound features involved herein constitute a family of features presenting a positive relief at their termination as they occur within the seismic data. The first family will obviously include the features rising within the Lower Eocene.

4-2-1 Description

The Lower Eocene displays numerous features distinguishing from each other by their sizes and extent. On seismic profile these features are characterized by their chaotic reflections, their depths range from 30 to 55 meters. The diameter of the structures mimicking their termination is comprised between 600 and 700 meters.

The shape is conic, cylindric or sub-cylindric. These features ascend from a stratigraphic level characterized by low amplitude reflections where their large roots are sometimes distinct from the surrounding setting. The flanks of these features exhibit dipping reflections. Some these reflections characterized by amplitude anomalies are V-shaped and are similar to those described by Løseth et al. (2003). At the south western part of the study area, survey ST0827 is characterized by two types of features terminating at different depths. The first types that emerge up to the intra-Oligocene surface are characterized by chaotic reflections. Their terminations are large, characterized by high amplitude reflections, and some of them take a mushroom-like shape meanwhile others tend to be less developed horizontally and are instead pronounced vertically by taking a viper's head- shape.

The features that exceed the intra-Oligocene surface consist of smaller chaotic columns pushing up the reflections. The features tend to be vertically elongated and consist of widespread high amplitude anomalies along the conduit all the way up.

The last family of columnar features include very small pipes characterized by chaotic reflections and that terminate at different level within the geological formations. Their

particularity is that they might terminate without being capped like their bigger counterparts or they merge with the bigger features or simply terminate when depression of the surface occur.

These features observable from the seismic profile and visualized in three dimensional view include crater-like depression features. On seismic profile they occur as push-down effect of the reflections. They are found either on top of noisy - seismic character' pipe that evolved deeper in the profile, or along fault trends mostly within the top Rogaland surface.

4-3 Features occurring between the seabed and intra-Oligocene

These features include pipes apparently stemming at the same stratigraphic level as those that terminate below or at the intra-Oligocene. Their roots are large compared with their terminations and present a chaotic seismic expression. These pipes interrupt the continuity of seismic reflections as they encounter reflectors and present an acute angle and up-bending (up-doming) effect at the places they seem to terminate. The stratigraphic levels where these structures terminate undergo two types of deformations including folds and faults. Folds mostly occur at the intra-Oligocene terminations meanwhile the reflectors such as Top Brygge is affected by both fold and faults and Opal A/Ct is dominated by faults. The pull-down effect affects the deeper horizons. They are more prominent within the shallower formations namely the Kai and Naust formations. The reflections are generally of low amplitude between the Opal A/CT reflections and the Top Kai reflections. However, localized high amplitude reflections are visible especially within the channels that seem to be the continuity of the pipes (Fig.4.5).

visible especially within the channels that seem to be the continuity of the pipes (Fig.4.5).

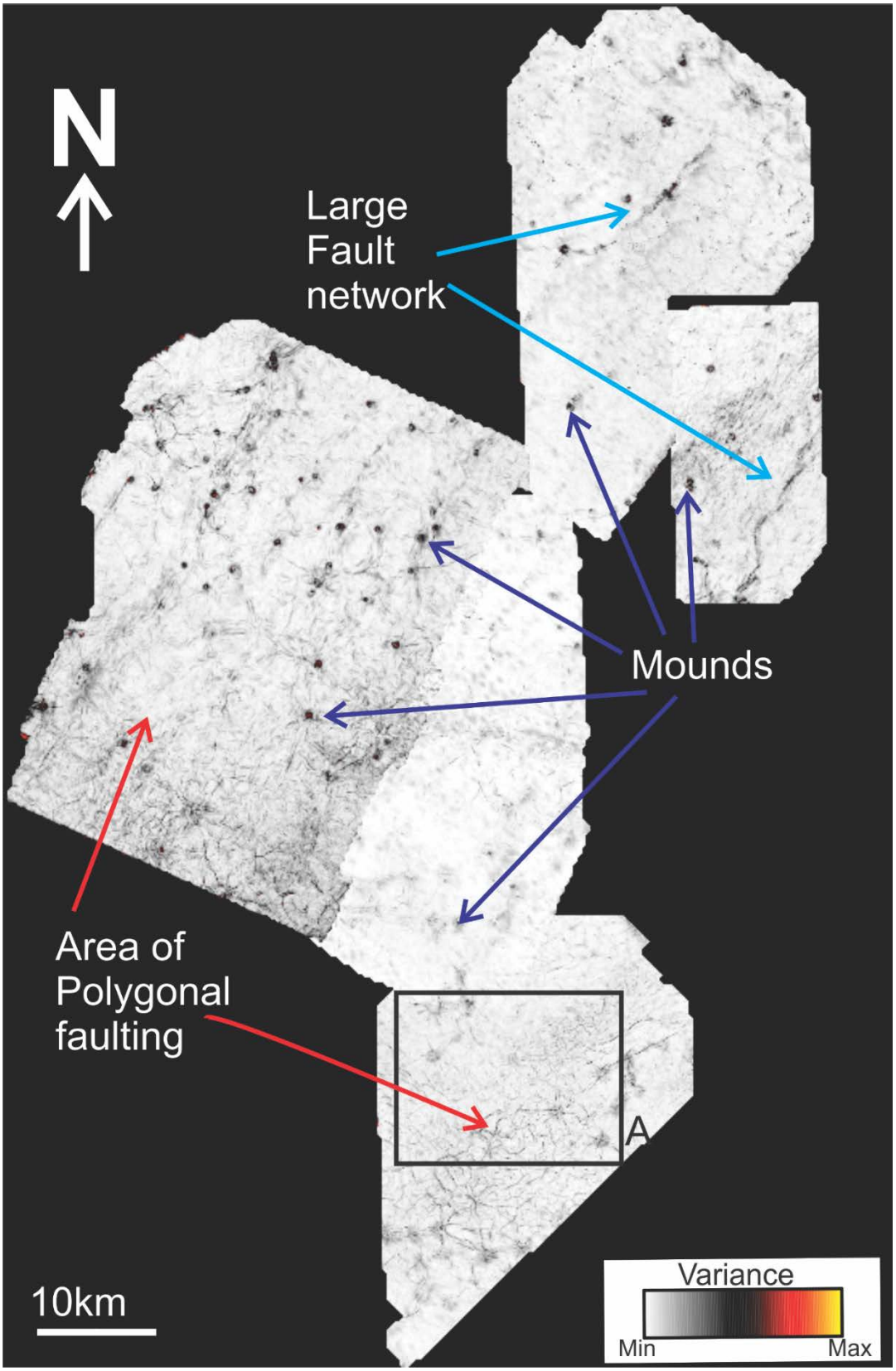

Figure 4.12 Variance attribute map, computed along the intra-Oligocene reflection, showing the spatial distribution of mounds and area polygonal faulting

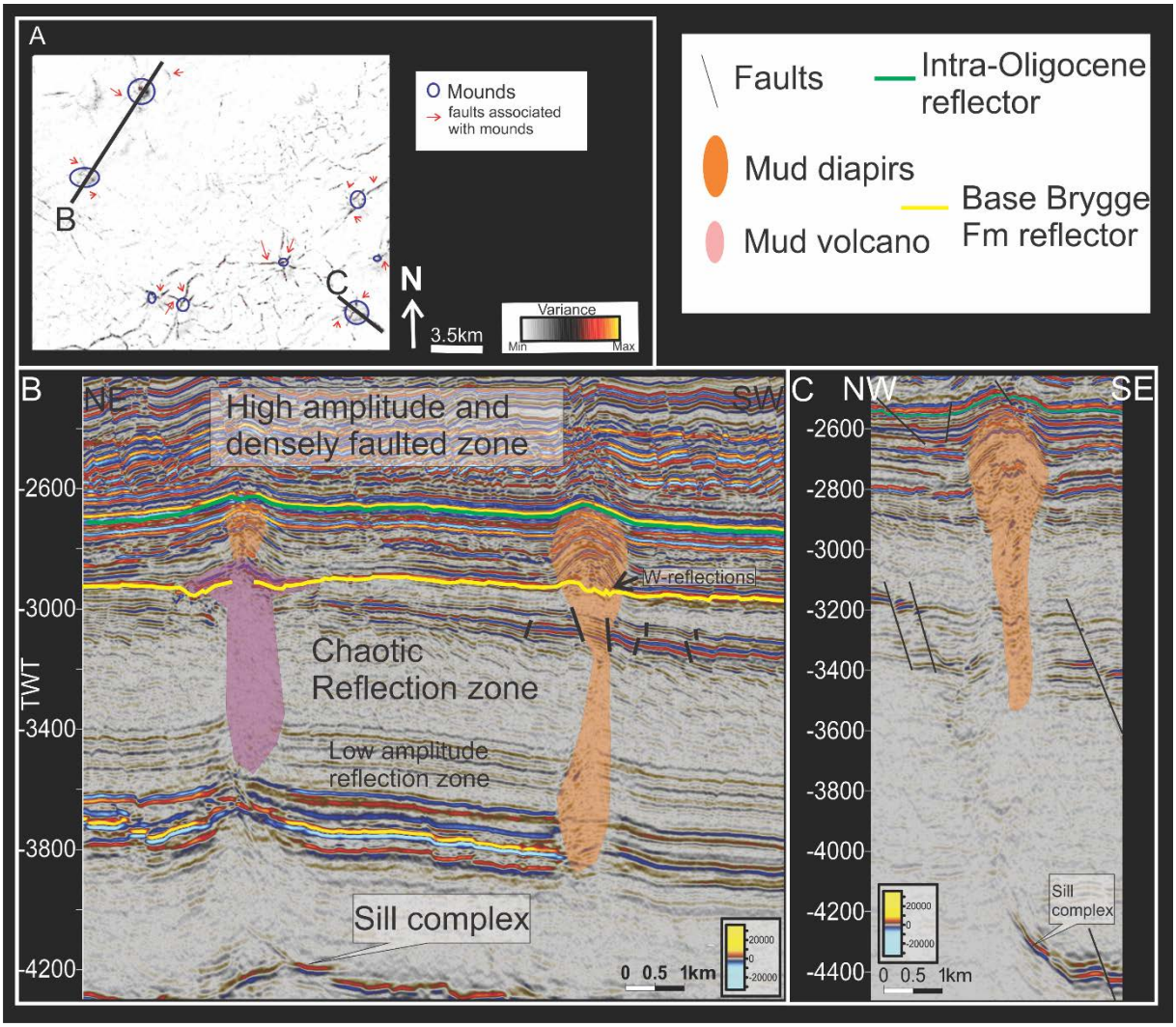

Figure 4.13 Spatial distribution of mounds and faults in **A)** and their seismic expression in **B)** and **C);** see figure 4.12 for the location of **A)**

5. DISCUSSION

5-1 Fluid Flow Features

The features described in the study area were observed in many locations including offshore and outcrops all over the world given that gas-seepage processes have been of high interest in the sedimentary basins (King and MacLean, 1970; Judd and Hovland , 2007, Heggland, 1997, 1998).

Previous studies carried out including in the study area and its vicinity in the Møre Basin led to the interpretation of these structures (Heggland, 1997, 1998; Hovland et al., 1998; Svensen et al., 2003; Planke et al., 2003; Svensen et al., 2003, 2004; Hansen et al., 2005, Dumke et al., 2014). Hansen et al. (2005) interpreted terminations that were observed and described in this study; they subdivided them in three types with respect to their shape.

The mushroom-shaped terminations observed and described in the present study were interpreted as mud laccoliths (Hansen et al., 2005). These features were reported to have emerged on the seafloor at the Paleocene /Eocene transition (Hansen et al., 2005). This shape is probably fostered by the emergence of fluidized products out of sedimentary formations, i.e the seabed, and the ability of the products to preferentially flow sideward once they emerged. Although the lithology of the mud laccoliths is not provided by well data, one can predict it mineralogy by assuming the fluids have bleached the formation around the conduit during their migration to the seabed (Judd and Hovland, 2007). The sediments mobilized during this process may therefore belong to deeper formations and/or derive from mineral precipitation because of a change in condition of temperature and pressure at the seabed (Judd and Hovland, 2007).

The viper's head – like features were ascribed to mud-diapirs (Hansen et al., 2005). This interpretation was driven by the intruding behavior of 'head' of these features in the base of the overlying Paleogene formations (Hansen et al., 2005). The occurrence of amplitude anomalies above some of these structures at shallower depths evidences fluid expulsion or leakage where terminations are affected by faults. Those faults therefore act as vertical fluid-migration pathways (Cartwright et al., 2007).

The small domes were suggested to represent mud-pillows (Hansen et al., 2005). The presence of gas or a difference in acoustic properties resulted from local differences in digenesis might be the cause of local high-amplitude reflections within the mud-pillows (Hovland and Judd, 1988).

The observations show that all the mounds that have been interpreted are linked to the deeper stratigraphic sequences by a vertical or sub-vertical conduit characterized by chaotic seismic reflections. Similar seismic facies were documented in volcano-sedimentary provinces including the mid-Norwegian margin (Svensen et al.,2003; Jamtveit et al., 2004; Planke et al., 2005) in the Faroe-Shetland (Grove, 2012) and regionally (NE Atlantic margin) (Hansen, 2006). These seismic facies are acknowledged identical in morphology to the field occurrences found in the Karoo Basin, South Africa (Jamtveit et al., 2004; Svensen et al., 2006). The features observed in vertical seismic sections were interpreted as vent complexes based on the morphology of the structures mounting the chimneys. Those structures were interpreted as mud-volcanoes as the vent mounds are eye-like structures (Planke et al., 2003; Svensen et al., 2003, 2004) or mud diapirs as the vent terminations are vertically elongated and pierce the base of the overlying stratigraphic unit (Hansen et al., 2005). The seismic amplitude anomalies associated with the conduit evidence the presence of gas in this case migrating upward. The study area displays

5-2 Giant Gjallar Vent (GGV)

This gigantic structure was termed Giant Gjallar Vent (GGV) and described as active feature rising at the present seafloor by gay et al. (2012) meanwhile previous studies in the area (Hansen et al., 2005) present the BPU as the paleo-seabed that underwent the extrusion activities of the unconsolidated sediments stemming from deeper horizons in order to form a mud volcano that they consider in the present days as buried, extinct and therefore inactive. Further studies in the area (Dumke et al., 2014) reveal more arguments advocating for the present activity of the two pipes that are meant to feed the structure that has emerged at the seafloor hence perpetuating the release of fluids in the water column. Although there is no clear evidence of fluid bubbles emanating from the structure at the seafloor the presence of seismic amplitude anomalies and localized phase reverse along the conduits indicating the upward migration of fluids.

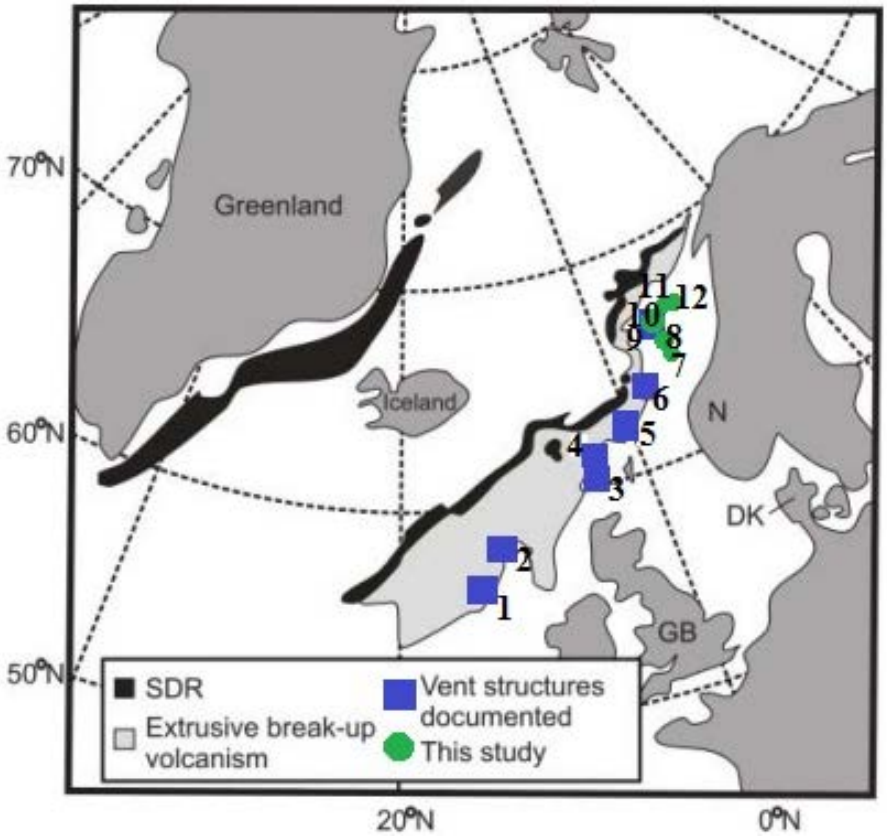

Figure 4.14 Map of the NE Atlantic margin showing areas where vents associated with sill emplacement have been documented during this and previous studies. 1, Rockall Trough: Joppen & White (1990). 2, NE Rockall Basin: Hansen (2006). 3, Central Faeroe–Shetland Basin: Hansen (2006). 4, Faeroe–Shetland Basin: Davies et al. (2002) and Trude et al. (2003). 5, Northern Faeroe–Shetland Basin: Hodges et al. (1999), Bell & Butcher (2002), Hansen (2006). 6, Møre Basin: Hansen (2006), Svensen et al. (2004) and Planke et al. (2005). 7, 8, 9, 10, 11, 12, Vøring Basin: Skogseid et al. (1992), Svensen et al. (2004) and Planke et al. (2005), This study (surveys SG9604, ST0827, GRE02, SH1002M11, ST0410). SDR, seaward-dipping reflectors (modified from Hansen, 2006).

Evidence of polyphasal fluid flow

The vent complexes occurring in the BPU reflectors are similarly characterized by the up-bending reflections in seismic section. At the bottom of the section, the vent conduits are apparently separated from the sill complexes occurring in the deeper stratigraphic level by a disturbed stratigraphic unit. Nevertheless the tips of the sills pointing upwards are surrounded by low amplitude down bending reflections and the chimneys display a concave root that can be extrapolated to the convex reflections occurring around the sill tips. This geometry suggests the buoyant fluids resulted from the overpressured zone are directed towards the conduits

(Hansen *et.*, 2005). Within the conduits the presence of high amplitude anomalies and v-shaped reflections are good evidence of upward fluid-migration (Løseth *et el.*, 2009). The continuous reflectors that are crossed by the geometry of the conduits are affected by faults all the way up. The mobilized mud making up the mud diapirs and volcano occurring around the BPU might have a short travel distance given that the stratigraphic unit between the Opal AC/T and BPU within the Kai Formation is made up of fine gained-sediment (Hansen *et al.,* 2005, Gay *et al.,* 2010). It's most likely that the faults within the conduits have play as migration path for the hydrothermal fluids resulted from the emplacement of sills in the basin (Svensen *et al.,* 2004, 2005).

The proximity of the roots of vent complexes emerging around the BPU and the sill tips suggests that the Cenozoic sediment were heated up as a result of volcanic intrusion (Planke *et al.*, 2005,). This pressure build up around the sills lead to the buoyancy of the pore fluid (Planke *et al.*, 2005; Hovland and Judd, 2007). The causality relationship between that episode of fluid flow and the volcanic intrusion within the study area can therefore be established. Two assumptions, regarding the occurrence of this phase of hydrothermal venting may arise. Firstly the venting occurred during the primary sill emplacement in the study area. The second assumption is that the vent complexes were put in place during previous hydrothermal activity in the study area and they have just been reactivated during later fluid migrations.

Figure 4.13B displays a mud volcano and mud diapir vertically related to each other. This relationship suggest that the formation of the mud volcano preceded the diapirism. The diapirism might have occurred during a later phase of fluid flow and mud mobilization from deeper unit and/or from the mud volcano.

The hydrothermal vent complexes were initially termed diatremes and volcanic necks by Du Toit (1904, 1912). The magma causes rapid heating of the sediments, and their pore fluids, that have undergone intrusion causing expansion and boiling of the pore fluids (Jamtveit et al, 2004) as well as metamorphic dehydration as a result of intrusive activity in sedimentary basins (Svensen et al, 2006). One of the consequences of these processes includes phreatic volcanic activity (Gevers 1928; Botha & Theron 1966; Coetzee 1966; Taylor 1970; Dingle et al. 1983; Seme 1997; Woodford et al. 2001) by the formation of cylindral conduits that pierce sedimentary strata all the way to the surface (Svensen et al, 2006). Hence the hydrothermal vents are pathways for gases produced in contact aureoles to the atmosphere, with the potential to induce climate changes (Svensen et al. 2004).

Sedimentary strata are dipping towards vent complexes from mud volcanoes and about 40 per cent of the hydrothermal vent complexes of offshore Mid-Norway (Planke et al. 2005). Phreatomagmatic eruptions are commonly associated with collapse and inward tilting of strata (Lorenz 1985; Svensen et al. 2004)

Recent studies have shown that hydrothermal vent complexes are widespread and spatially associated with sill intrusions at depth in the Møre and vøringg basins of offshore Norway (Fig.4.15) (Jamtveit et al. 2004; Svensen et al. 2004; Planke et al. 2005; Svensen et al. 2006).

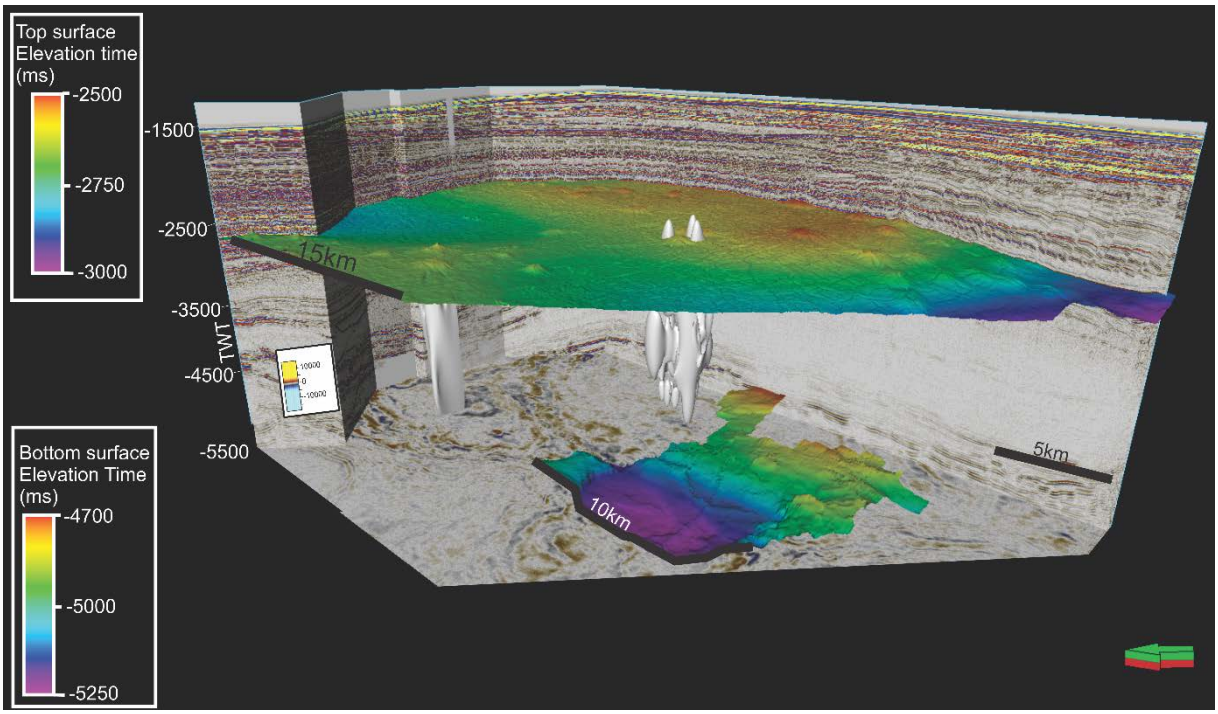

Figure 4.15 3D visualization of features in the study area. With vertical features are vent complexes.

6. CONCLUSION

On the basis of the results from the dataset in presence, it could be concluded that:

- The study area has undergone episode of fluid flow;
- Volcanic intrusions in the basin created significant perturbation in the sedimentary strata;
- Mud mobilized used different paths to migrate upwards namely faults fractures;
- Hydrothermal venting I the basin was triggered by sills.

7. REFERENCES

Apps, J. A. and Kamp, P. C. van de, 1993. Energy gases of abiogenic origin in the Earth's crust. In *The Future of Energy Gases*. United States Geological Survey, Professional Paper 1570, 81–132.

Becker, K., the Leg 174B Scientific Party, and Davis, E. E., 1998. Leg 174B revisits Hole 395A: logging and long-term monitoring of off-axis hydrothermal processes in young ocean crust. *JOIDES Journal*, 24(1),

Berndt, C., Mienert, J., Vanneste, M., Bünz, S., and Bryn, P., 2001. Submarine slope-failure offshore Norway triggers rapid gas hydrate decomposition. Proceedings of the Fourth International Conference on Gas Hydrates,Yokohama, May 19–23.

Binns, R. A., Barriga, F. J. A. S., Miller, D. J., and the Shipboard Scientific Party, 2001. The third dimension of an active back-arc hydrothermal system: ODP Leg 193 at PACMANUS. EOS – Transactions of the American Geophysical Union, 82, Fall Meeting Supplement, abstract F587.

Blystad, P., Brekke, H., Færseth, R.B., Larsen, B.T., Skogseid, J., Tørudbakken, B., 1995. Structural elements of the Norwegian continental shelf. Part II: the Norwegian Sea Region. Norwegian Petroleum Directorate. Bulletin 8.

Boorman, S.J., McGuire, J.B., Boudreau, A.E. & Kruger, F.J. 2003. Fluid overpressure in layered intrusions: formation of a breccia pipe in the Eastern Bushveld Complex, Republic of South Africa. Mineralium Deposita, 38, 356 – 369.

Bottinga and Weill, 1972, Viscosity of Magmatic Silicate Liquids A model for calculation, AJS 272, 438-475.

Butterfield, D. A., 2000. Deep ocean hydrothermal vents. In Sigurdsson, H. (ed.), *Encyclopedia of Volcanoes*. New York, Academic Press, pp. 857–75.

Cartwright, J., Huuse, M., Aplin, A., 2007. Seal bypass systems. AAPG Bulletin 91, 1141–1166.

Chevalier L, Woodford A (1999) Morph-tectonics and mechanism of emplacement of the dolerite rings and sills of the western Karoo, South Africa. S Afr J Geol 102:43–54.

Coetzee, C.B. 1966. An ancient volcanic vent on Boschplaat 369 in the Bloemfontein district, Orange Free State. Transactions of the Geological Society of South Africa, 69, 127–137.

Dalland, A., Worsley, D. and Ofstad, K. (eds.) 1988: A lithostratigraphic scheme for the Mesozoic and Cenozoic succession offshore mid- and northern Norway. NPD-Bulletin No. 4, 65 pp.

Davies, R.J., Stewart, S.A., 2005. Emplacement of giant mud volcanoes in the South Caspian Basin: 3D seismic reflection imaging of their root zones. Journal of the Geological Society 162, 1–4.

DELANEY, P.T. 1982. Rapid intrusion of magma into wet rocks: groundwater flow due to pore pressure increases. *Journal of Geophysical Research*, 87, 739-7756.

Du Toit AL (1920) The Karoo dolerite of South Africa: a study of hypabyssal injection. Trans Geol Soc S Afr 23:1–42.

Eidvin, T., Bugge, T., Smelror, M., 2007. The Molo Formation, deposited by coastal progradation on the inner Mid-Norwegian continental shelf, coeval with the Kai Formation to the west and the Utsira Formation in the North Sea. Norwegian Journal of Geology 87, 75–142.

Eldholm, O., Thiede, J., Taylor, E., 1989. Evolution of the Vøring Volcanic Margin. In: Eldholm, O., Thiede, J., Taylor, E. (Eds.), Proceedings of the Ocean Drilling Program, Scientific Results, 104, pp. 1033–1065.

Faleide, J.I., Solheim, A., Fiedler, A., Hjelstuen, B.O., Andersen, E.S., Vanneste, K., 1996. Late Cenozoic evolution of the western Barents Sea-Svalbard continental margin. Global and Planetary Change 12, 53–74.

Faleide, J.I., Tsikalas, F., Breivik, A.J., Mjelde, R., Ritzmann, O., Engen, Ø., Wilson, J., Eldholm, O., 2008. Structure and evolution of the continental margin off Norway and the Barents Sea. Episodes 31, 82–91.

Francis EH (1982) Magma and sediment-I. Emplacement mechanism of the late Carboniferous tholeiite sills in the northern Britain. Geol Soc Lond 139:1-20.

Francis EH, Walker BH (1986) Emplacement of alkali-dolerite sills relative to extrusive volcanism and sedimentary basins in the Carboniferous of Fife, Scotland. Trans R Soc Edinb 77: 309 – 323.

Fyfe, W. S., 1992. Magma underplating of continental crust. Journal of Volcanology and Geothermal Research, 50, 33–40.

Fyfe, W. S., 1994. The water inventory of the Earth: fluids and tectonics. In Parnell, J. (ed.), Geofluids: Origin, Migration and Evolution of Fluids in Sedimentary Basins. Geological Society of London, Special Publication 78, 1–7.

Gay, A., Berndt, C., 2007. Cessation/reactivation of polygonal faulting and effects on fluid flow in the Vøring Basin, Norwegian Margin. Journal of the Geological Society 164, 129–141.

Gay, A., Mourgues, R., Berndt, C., Bureau, D., Planke, S., Laurent, D., Gautier, S., Lauer, C., Loggia, D., 2012. Anatomy of a fluid pipe in the Norway Basin: initiation, propagation and 3D shape. Marine Geology 332–334, 75–88.

Hannum, C. 1980. Sandstone and conglomerate–breccia pipes and dikes of the Kodachrome Basin area, Kane County, Utah. Geology Studies, Brigham Young University, 27, 31–50.

Hansen, J.P.V., Cartwright, J.A., Huuse, M., Clausen, O.R., 2005. 3D seismic expression of fluid migration and mud remobilization on the Gjallar Ridge, offshore mid-Norway. Basin Research 17, 123–139.

Hjelstuen, B.O., Eldhom, O & SKOGSEID, J (1997) Vøring Plateau diapir fields and their structural and depositional setting. *Mar. Geol.*, 144, 33-57.

Hovland, M., Nygaard, E., Thorbjørnsen, S., 1998. Piercement shale diapirism in the deep water Vema Dome area, Vøring basin, offshore Norway. Marine and Petroleum Geology 15, 191–201.

Hustoft, S., Bünz, S., Mienert, J., 2010. Three-dimensional seismic analysis of the morphology and spatial distribution of chimneys beneath the Nyegga pockmark field, offshore mid-Norway. Basin Research 22, 465–480.

Isaksen, D. and Tonstad, K. (eds.) 1989: A revised Cretaceous and Tertiary lithostratigraphic nomenclature for the Norwegian North Sea. NPD-Bulletin No. 5, 59 pp.
Jansen, E., Sjøholm, J., 1991. Reconstruction of glaciation over the past 6 Myr from ice-borne deposits in the Norwegian Sea. Nature 349, 600–603.

Judd, A. & Hovland, M. (2007). Seabed fluid flow – impact on geology, biology and the marine environment. Cambridge University Press, Cambridge, pp 400. www.cambridge.org.

Kenkmann, T. 2003. Dike formation, cataclastic flow, and rock fluidization during impact cratering: an example from the Upheaval Dome structure, Utah. Earth and Planetary Science Letters, 214, 43–58.

Kurszlaukis, S., Buttner, R., Zimanowski, B. & Lorenz, V. 1998. On the first experimental phreatomagmatic explosion of a kimberlite melt. Journal of Volcanology and Geothermal Research, 80, 323–326.

Leaman DE (1975) Form, mechanism, and control of dolerite intrusion near Hobart, Tasmania. J Geol Soc Aust 22:175–186.

Lorenz, V., 1975. Formation of phreatomagmatic maardiatreme volcanoes and its relevances to kimberlite diatremes. *Physics and Chemistry* of the Earth, 9, 17–27.

Lowe, D.R. 1975. Water escape structures in coarse-grained sediments. Sedimentology. 22, 157-204.

Løseth, H., Henriksen, S., 2005. A Middle to Late Miocene compression phase along the Norwegian passive margin. In: Doré, A.G., Vining, B.A. (Eds.), Petroleum Geology: North-West Europe and Global Perspectives — Proceedings of the 6th Petroleum Geology Conference, Geological Society, London, pp. 845–859.

Navikov, L.A. & Slobodskoy, R.M. 1979. Mechanism of formation of diatremes. International Geology Review, 21, 1131–1139.

Ottesen, D., Rise, L., Andersen, E.S., Bugge, T., Eidvin, T., 2009. Geological evolution of the Norwegian continental shelf between 61 N and 68 N during the last 3 million years. Norwegian Journal of Geology 89, 251–265.

P. M. Tucker, 1988 Society of Exploration Geophysicist.

Planke, S., Rasmussen, T., Rey, S.S., Myklebust, R., 2005. Seismic characteristics and distribution of volcanic intrusions and hydrothermal vent complexes in the Vøring and Møre basins. Geological Society, London, Petroleum Geology Conference Series 6, 833–844.

Podlachnikov & Wickham 1994. Crystallizationof hydrous magmas: calaculation of associated thermal effects, volatile fluxes, and isotopic alteration. *Journal of Geology*, 102, 25-45.

Ren, S., Faleide, J.I., Eldholm, O., Skogseid, J., Gradstein, F., 2003. Late Cretaceous–Paleocene tectonic development of the NW Vøring Basin. Marine and Petroleum Geology 20, 177–206.

Shoulders, S.J. & Cartwright, J. 2004. Constraining the depth and timing of large-scale conical sandstone intrusions. Geology, 32, 661–664.

Smallwood JR, Maresh J (2002) The properties, morphology and distribution of igneous sills: modelling, borehole data and 3D seismic data from the Faeroe-Shetland area. In: Jolley DW,

Bell BR (eds) The North Atlantic Igneous Province: Stratigraphy, tectonic, volcanic and magmatic processes. Geol Soc Lond Spec Pub 197:271–306.

Svensen, H., Planke, S, Malthe-Sørensen, A., Jamtveit, B., Myklebust, R., Rasmussen, T. & Rey, S.S. 2004. Release of methane from a volcanic basin as a mechanism for initial Eocene global warming. *Nature,* 429. 542-545.

Svensen, H., Planke, S., Jamtveit, B., Pedersen, T., 2003. Seep carbonate formation controlled by hydrothermal vent complexes: a case study from the Vøring Basin, Norwegian Sea. Geo-Marine Letters 23, 351–358.

Symonds, P. A., Planke, S., Frey, Ø. & Skogseid, J. 1998. Volcanic development of the Western Australian continental margin and its implications for basin development. In: Purcell, P. G. & Purcell, R. R. (eds) The Sedimentary Basins of Western Australia 2: *Proceedings of Petroleum exploration Society of Australia Symposium,* Perth, 33-54.

Vail, P.R., Hardenbol, J., 1979. Sea-level changes during the Tertiary. Oceanus 22, 71–79.

Wood MV, Hall J, Doody JJ (1988) Distribution of early Tertiary lavas in the NE Rockall Trough. In: Morton AC, Parsons LM (eds) Early Tertiary volcanism and the opening of the NE Atlantic. Geol Soc Lond Spec Publ 39:283–292.

Woodford, A.C., Botha, J.F. & Chevallier, L. et al. 2001. Hydrogeology of the main Karoo Basin: Current Knowledge and Research Needs. Water Research Commission Pretoria, Report, 860.

Woolsey, T.S., McCallum, M.E. & Schumm, S.A. 1975. Modeling of diatreme emplacement by fluidization. Physics and Chemistry of the Earth, 9, 29–42.

www.npd.no

Yilmaz (2001) Seismic data analysis processing, inversion and interpretation of seismic data. Soc Explor Geophys Tulsa, 2,027 pp.